Design and Development of FingerTac: A Wearable Tactile Sensor and its integration with ExoGlove for Position Measurement

FingerTacの設計と開発：手先位置測定のためのウェアラブル触覚センサとExoGloveの統合

2024/02

Prathamesh Prasad SATHE
サテ　プラスメシュ　プラサド

Design and Development of FingerTac: A Wearable Tactile Sensor and its integration with ExoGlove for Position Measurement

FingerTacの設計と開発：手先位置測定のためのウェアラブル触覚センサとExoGloveの統合

2024/02

Waseda University Graduate School of Creative Science and Engineering

Department of Modern Mechanical Engineering, Research on Intelligent Machines

Prathamesh Prasad SATHE
サテ　プラスメシュ　プラサド

Abstract

Sathe Prathamesh Prasad

Design and Development of FingerTac: A Wearable Tactile Sensor and its integration with ExoGlove for Position Measurement

The dexterity of the human hands allows humans to create fine works of art. Normally these works of art can be preserved in museums and world heritage sites. These works of art have been created by artists which speak for a country's rich cultural heritage. Some of the art forms are still practiced today such as calligraphy while some have been endangered such as the art of ukiyo-e. Due to massive industrialization and changing lifestyles these artworks have been diminishing throughout the time. The Major driving force behind the creativity of these works of arts is the dexterity of the human hands. Dexterity has empowered ancient artisans to create beautiful works of art even in the absence of advanced technology. Thus, as a first step, to preserve the rich cultural heritage of a country we must extract the essence of human hand dexterity. Essence of human hand dexterity can be divided into three parts first part is the application of 3-axis force on an object. The second part is the measurement of finger posture and the third part is the fine motor skills required to manipulate an object. Thus this doctoral thesis proposes a combined distributed 3-axis force and position measurement solution to extract the essence of human hand dexterity. Initially a wearable tactile sensor which is able to measure forces without covering the palmar side of the fingertip is improved by integrating it with the first version of a ExoGlove. The first version of the ExoGlove is able to measure the joint angle between finger segments and allows the user to measure the finger posture. The ExoGlove version 1 also support the sensors while manipulating an object. However due to the physical characteristics of the sensor the

sensor cannot be used for measuring 3-axis forces distributed over the fingertip area as the sensor provides 3 axis measurement at single point on the fingertip. To address this drawback we propose FingerTac- distributed 3-axis wearable sensor which can measure force across the fingertip area. The sensor is able to be worn easily on the fingertips of the user. The sensor allows the user to interact with the object indirectly while interacting with the object. This sensor solves the first essence of human dexterity as it is able to measure distributed 3-axis force around the fingertip area. To extract the second and third essence of human hand dexterity, the FingerTac is integrated with the ExoGlove Version 2. The ExoGlove is equipped with Hall-Effect based encoders which have been designed to be embedded in the revolute joints of the ExoGlove. Overall the ExoGlove consists of a Four Degree of Freedom articulated linkage mechanism which is able to tract the position and orientation of the FingerTac while manipulating an object.

Acknowledgments

I would like to express my sincere gratitude to Professor Shigeki Sugano for accepting me to become a graduate student of Waseda University and become a part of his laboratory. I would like to thank him for dedicating his valuable time for discussing several important points in my research and providing me valuable feedback on my research despite his busy schedule throughout my years of Marsters and Doctoral courses. The journey of my doctoral research would have been impossible without his unwavering support.

I would like to thank Professor Alexander Schmitz who introduced me to the concept of tactile sensors. I would like to thank him for guiding me and providing valuable feedback and support to conduct my research in tactile sensors and robotics. I would like to also thank him for teaching me how to write research papers at the same time I would like to extend my gratitude to him for proofreading my research papers and for providing valuable feedback for the same.

I would like to thank my friends, colleagues and members of the sensor team, Dr. Tito Tomo Pradhono, Dr. Sophon Somlor, for teaching me about embedded hardware development. I would like to thank my best friends Jagjit Singh and Dr. Shardul Kulkarni, for always being there during tough times, for helping in software development and supporting me throughout my memorable time of masters and Doctoral courses.

Furthermore, I want to express my heartfelt thanks to my family members – my father Prasad Sathe, my mother Rupashree Sathe, my uncle Dr. Aditya Sathe, my aunt Dr. Pragati Sathe, my cousin sister Mihika Sathe, and my grandmother Anuradha Sathe. They have been a continuous source of inspiration and support throughout the journey of my Master's and Doctoral courses at Waseda University. I thank them for their guidance during tough times and for always being there for me. Finally, I would like to thank my fiancée Dr. Aashlesha Marathe for being my better half and supporting me throughout my doctoral journey.

Table of Contents

Table of Figures

Chapter 1

Introduction

1.1 Background - Creativity in hand of ancient artisans:

Since the last known history of mankind, humans have been designing and creating various tangible and traditional works of art. These traditional artworks can be found in the form of temple carvings, as well as in everyday items like pottery. Unfortunately, many such artworks have been lost to history, primarily due to the destructive actions of humans, such as war. Others have succumbed to the destructive forces of nature, such as earthquakes, floods, landslides, etc. Interestingly, these natural calamities have, at times, acted as preservers, burying these arts within the earth's crust.

Some of these artifacts have been rediscovered through excavations, while many beautiful works of art remain lost to time. The ones that have been unearthed are often exhibited in museums, and some of the discovered artworks have earned the status of world heritage sites, thereby being intrinsically preserved for future generations.

The artworks exhibited in heritage sites and museums speak not just of the creativity but also of various aspects of human life and answer various questions such as the overall status of the lifestyles of ancient humans, how technologically advanced they were at the time etc. These artifacts showcase their harsh living conditions and speak for the difficulties faced by ancient humans for living their lively hood. Moreover, these artifacts are a testament to human creativity and speak for the capacity of humans to achieve greater feats of creation through boundless exploration of their imagination and relentless pursuit of innovation.

Different artifacts have been discovered in different parts of the world speaking

volumes about different cultures and traditional practices. We must take inspiration from these creative artifacts to gain a larger understanding of what drives human creativity.

Let us look at some of the examples of historical artifacts and view them in the lens of human creativity and understand the methods utilized to drive human creativity forward.

1.1.1 Lion-man of the Hohlenstein-Stade:

The oldest known artifact discovered is the “Löwenmensch Figurine or Lion-man of the Hohlenstein-Stade” as shown in the Fig. 1.1 below.

Fig.1.1. Lion-man of the Hohlenstein-Stade

This artifact was carved out of ivory and was discovered in Hohlenstein-Stadel Cave, Swabian Jura in Germany. This artifact was known to have been created around 40,000 BCE. This shows that human creativity was not only developed but also it was

flourishing around the year 40,000 BCE even if there was an absence of modern technology.

1.1.2 Kailash Temple of Ajanta Elora Caves:

The magnanimity of human creativity can be realized by visiting the Kailash Temple situated in the Ajanta-Elora caves as shown in the Fig. 1.2 below. Archeologists have discovered that this temple has been carved entirely out of a solid rocky mountain.

Fig 1.2. Kailash Temple in Ajanta-Elora Caves

Archeologist state that the statues in the Kailash temple are also carved out of stone rocks. This temple and its carvings are known to have been created around 756 - 773 CE. The marvel of the Kailash Temple at the Ajanta Ellora Caves lies in the fact that the entire structure has been meticulously carved out from top to bottom from a single solid rock. This speaks volumes about the level of human creativity during the period of 756 - 773 CE Asia. It's astonishing to realize that these rocks were entirely sculpted by artisans using their hands, employing simple tools and techniques. This shows that during the period of 756 - 773 CE the Asian civilization have mastered the creativity

domain and without the help of modern technology were able to carve out such beautiful works of arts.

Ajanta-Elora caves has been designated as a UNESCO heritage site and this site attracts tourists from all parts of the world to visit and view these locations to gain inspiration from the magnificent sculptures created by ancient humans.

1.1.3 Thirty-Six views of Mount Fuji by Hokusai:

Some of the most famous works of traditional Japanese art is the art of ukiyo-e or wooden block prints. One of Japan's most famous ukiyo-e painters, Hokusai painted the Thirty-Six Views of Mount Fuji on wooden block prints. One of his paintings illustrates the large-scale tsunami that is being viewed from the ocean with the calm and serene backdrop of Mount Fuji at a distance be seen in the Fig. 1.3. below.

Fig 1.3. Kanagawa Oki Uranami

The wave has believed to be struck the Kanagawa Harbour hence Hokusai named this painting as the Kanagawa Oki Uranami - “The Hollow of the Deep- Sea Wave off Kanagawa”

These paintings are known to be created between 1760 to 1849 AD. It is evident that advanced printing technologies did not exist during the time of 1700s in Japan and yet painters and artists were able to create such beautiful paintings with eye-catching color combinations. It should be noted that laying of a uniform color on a canvas may seem to be simple however, it requires high level of hand - eye coordination of the painter. Also laying fine strokes of paint on a canvas to create beautiful curves by using simple tools like a paint brush brings to life the creativity in an artist’s hands. Fine movements generated by the artists hand are often overlooked but are very important in creating beautiful works of arts.

Overall, we must appreciate these paintings as they are also a testament to human creativity and function as evidence that even in the absence of advanced technology humans can create beautiful art works just by using their hands.

1.1.4 Hoke-Gisho oldest Japanese Calligraphy:

Calligraphy is Japan’s one of the most oldest form of art. The Japanese prince, Shotoku has written Japan’s oldest known calligraphy script known as Hokke Gisho as shown in the Fig. 1.4. Archeologists claim that Hoke-Gisho has been scripted sometime during the 7^{th} century in ancient Japan. It is the oldest known Japanese text.

Calligraphy can be dismissed simply as a form of writing old Japanese Kanji characters however it is a much-evolved skill from ancient to modern-day Japan. Japanese Calligraphy takes extreme patience to master as it is considered one of the

most difficult skills to acquire.

It should be noted that making fine movements with the brush and drawing relatively similar strokes on the Calligraphy paper can seem to be simple however requires a high level of coordination between calligrapher fingertips. The effective way of handling the brush by the Calligraphy artist is a testament to creativity of humans and its effect on modern-day tasks.

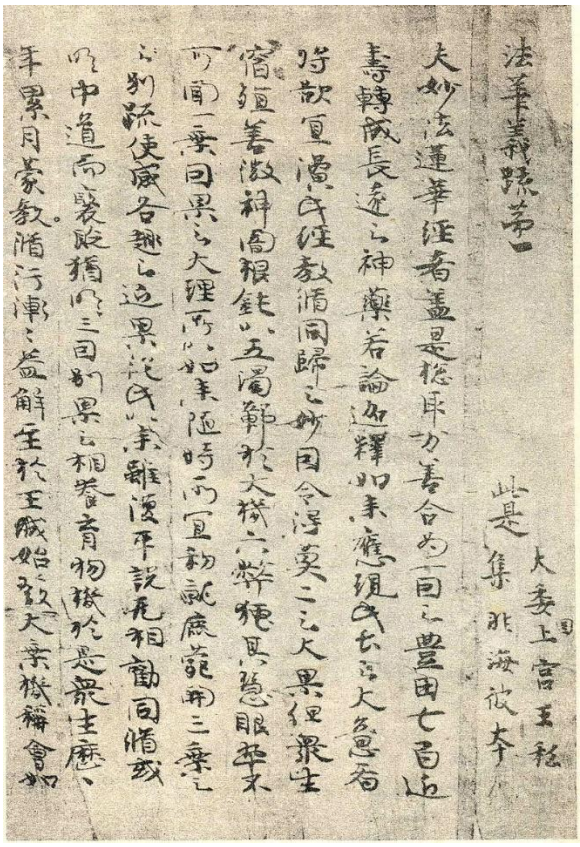

Fig 1.4. Japanese Calligraphy by Prince Shotoku

While Western calligraphy has been on a decline over the ages, Japanese Calligraphy is still practiced today as being one of the oldest forms of traditional craft.

Ancient works of art serve as a showcase of the primitive technology employed during their respective periods. Furthermore, these artworks were created by the skilled

artists using their hands, highlighting the craftsmanship and techniques mastered by these individuals. It must be noted that these works of art even though primitive can be effectively competing with the modern-day art as the skills used by ancient humans are unmatched as compared with modern artist using modern tools. It must be noted that human hands are at the helm of human creativity and are an effective tool driving human creativity forward. I believe that the dexterity of the human hands compensated for the limitation of the technology during ancient times.

1.2 Preservation of Traditional works of art:

Some traditional crafts, like sculpting, calligraphy, pottery, and painting, have withstood the impact of modern industrialization, while many other crafts have faded away over time. For example, in India during the festival of Ganesh Chaturthi, many artisans are tasked with sculpting idols of lord Ganesh as shown in the Fig. 1.5 below.

Fig 1.5. Modern day artist sculpting Ganesh Idols for Ganesh Chaturthi festival

These idols are sculpted using various materials such as plaster of paris, clay, and mud. The tradition of sculpting Ganesh idols is very old but has survived through the wrath of time and modern industrialization. However, one must note that this tradition is also susceptible to decline due to massive industrialization. Overall, all traditional works of art along with their techniques have been on the decline all over the world as presented in the literature [1.1].

For example, in Japan due to massive industrialization and changing lifestyle

demands, handmade traditional crafts are on decline as shown in the Fig.1.6 below.

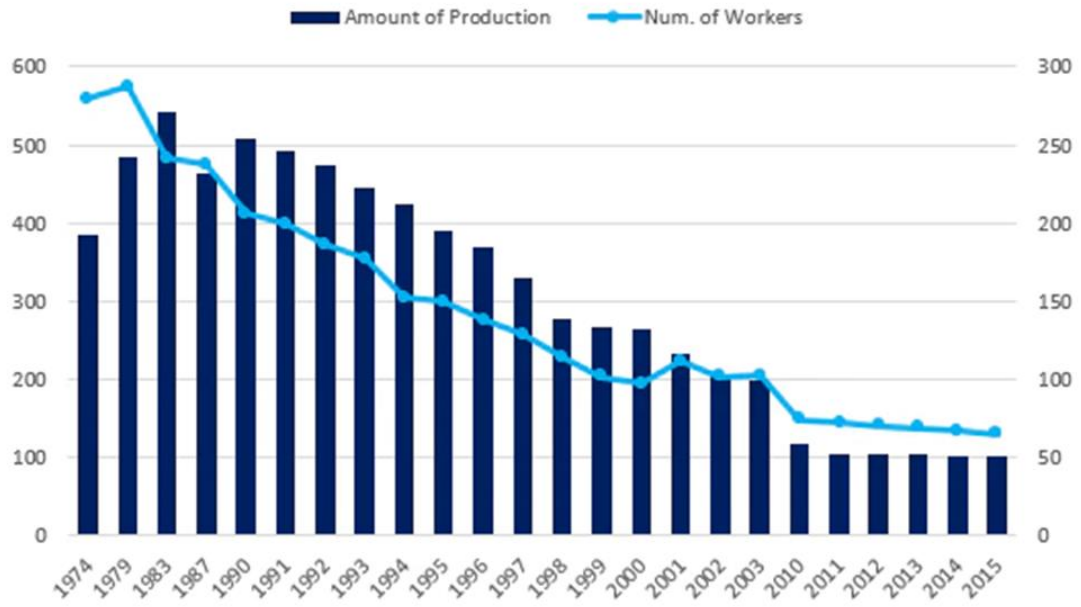

Fig 1.6. Decline in traditional craftsmen who specialize in traditional handicrafts

The graph points to the decrease in the number of skilled traditional craftsmen who specialize in traditional handicrafts. Dynamic urban lifestyles has brought a strong demand for mass production of various items. Nowadays even traditional works of art are mass produced in large factories. This has threatened traditional artists along with their skill sets.

Traditional works of art speaks for a country's rich cultural heritage. The more beautiful and advanced the techniques and skills used to create the art the more richer the culture is of a country. Techniques used in creating these crafts show how advance these cultures were during the particular era. Overall, traditional works of art are an important aspect of the cultural heritage of the human civilization and must be safeguarded or preserved.

1.3 Dexterity of Human Hands:

It must be noted that the above mentioned works of art have been created by artists just by their hands using simple tools and techniques. The human hand plays an important role in handling various objects. This literature describes the evolution of dexterity [1.3]. Overall dexterity of the human hands plays an important role in driving human creativity. The dexterity of the human hands has allowed artists to hold and manipulate the tool in different postures as shown in the Fig 1.7. Thereby allowing the artist to create fine works of art. Fig 1.8 shows different tools utilized by the artist to create different handicrafts.

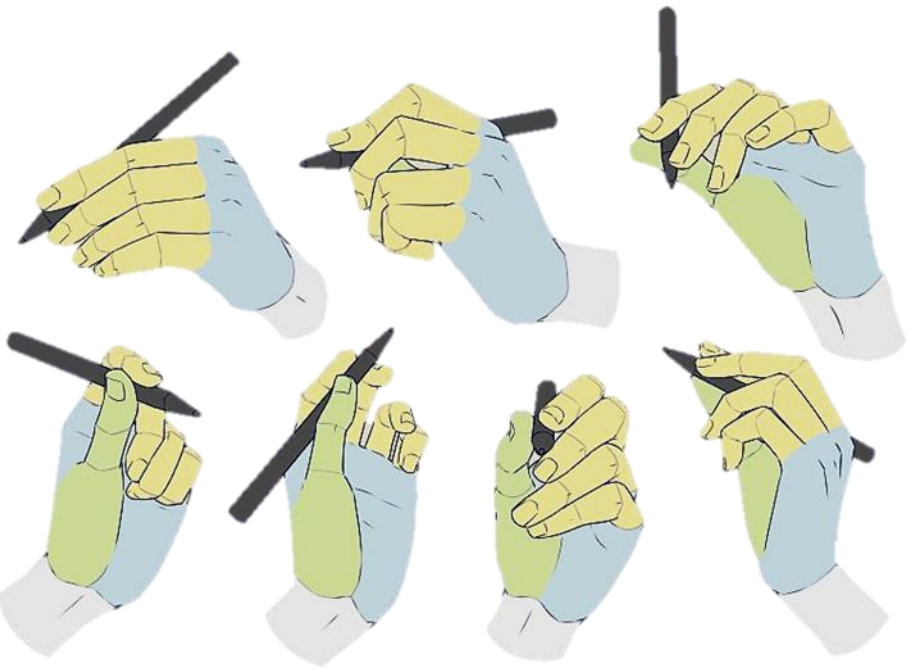

Fig 1.7 Dexterity of the human hand allows humans to manipulate the tool

Moreover, it must be noted that the dexterity of the human hand empowers the artist to create these works of arts. The way in which the artist uses the dexterity of his or her hand to create fine strokes while painting or the gentleness used while carving is what which creates beautiful statues or painting. The combination of dexterity of the human hand and the skill of the artist pours life into the handmade artifacts.

Fig 1.8 Dexterity of the human hand empowers artists to create handicrafts.

1.3.1 Mechanoreceptors function as tactile sensors:

The remarkable dexterity of the human hand and the ability to perform fine manipulations enables secure handling of objects of varying properties, shapes and sizes. This literature illustrates the mechanics involved in tactile sensation for humans [1.4]. The human hand's palmar side is equipped with fine mechano-receptors as shown in the Fig 1.9 to sense the objects in physical space. The tactile skin of the human's hand plays a major role in fine manipulation of different objects. The tactile skin allows the humans to estimate the basic physical properties of the object such as weight and stiffness of the object. This allows the human hand to perform various types of fine manipulation tasks. Delicate tasks such as folding a paper with precision to holding an egg without breaking it are some of the examples of the fine manipulation tasks. The human hand is also able to work on precision tasks such as threading a needle with hand-eye coordination. Fine

manipulation tasks performed by human hands seem simple however it should be noted that these tasks involve intricate multi modal coordination of tactile touch and vision.

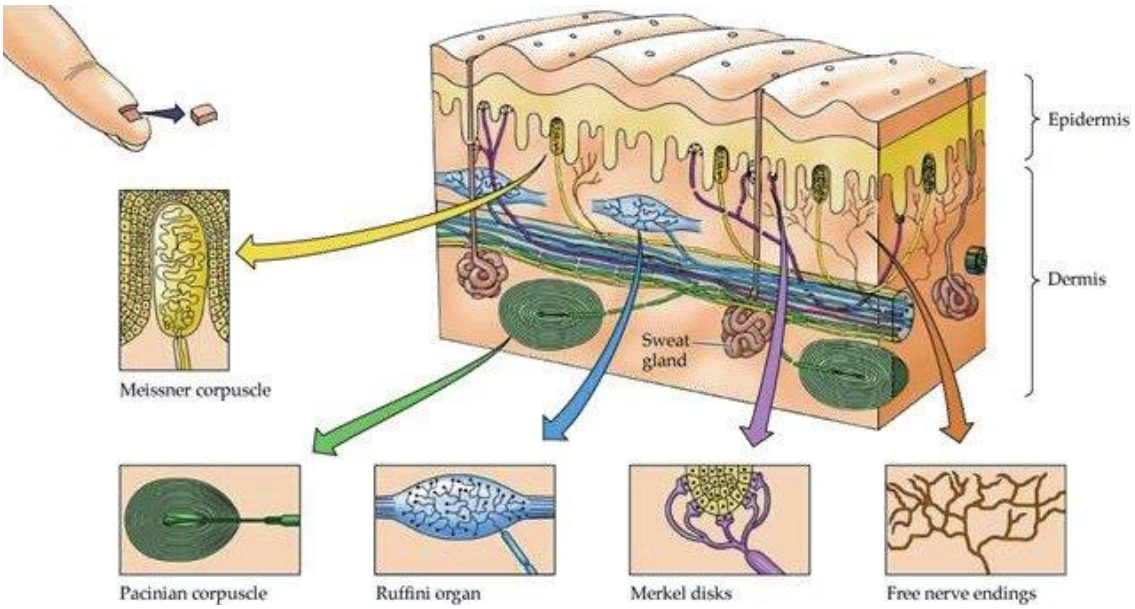

Fig 1.9 Mechano receptors in fingertips allows humans to feel objects.

In order for collaborative robots to perform similar human like tasks while working in close cooperation with human workers we must understand that it is essential for robot hands to have object handling skills similar to that of the humans. Even simple tasks as mentioned above require not even hand eye coordination but also require tactile information to interact with the external objects. Also, it must be emphasized that in order for the human robot cooperation to be successful the robot hand should have the ability to effectively and safely handle objects which are designed for humans and which are handled by humans on a daily basis. In order for the robot hands to handle the objects effectively and efficiently and perform human-like motion we must learn how humans interact with different objects using human hands.

1.3.1 Essence of Human Hand Dexterity:

Several research literatures dissect the importance of dexterity for handling different objects [1.5], [1.6], [1.7], [1.8]. It describes how humans use the dexterity of their hands as a tool to perform various tasks. Overall, the dexterity of the artist's hands can be divided into three major parts as listed below. Essence of dexterity can be pictorially represented as the following Fig.1.10. the red arrows represent the 3-axis force applied by the artist to handle the calligraphy brush. The blue lines represent the finger posture to handle the calligraphy brush.

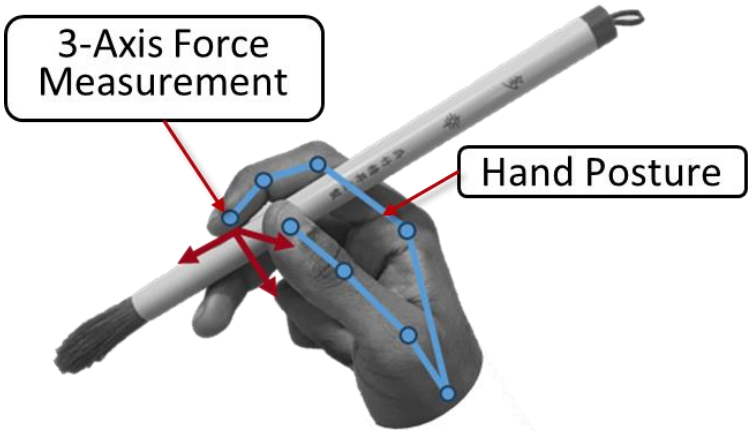

Fig 1.10 Dexterity of the Calligraphy artists hands.

1. Tool Grasping Force:

Tool Grasping force is the force used to grasp the tool while manipulating the tool in the human hand workspace. The figure below shows a calligraphy artist holding the calligraphy brush. In this case the tool grasping force will be the force used for grasping the calligraphy brush.

2. Finger Posture while holding the tool:

The artists hold the calligraphy brush in certain posture while performing strokes on the canvas or carving wooden blocks. This posture forms the basis of tool manipulation and is an important to perform stable grasp of the tool while

performing the art.

3. Fine motor skills for tool manipulation:

Fine motor skills of the human hand are used to dynamically change the posture of the tool constantly over time to perform a certain operation such as fine strokes on the canvas. In the case of calligraphy, the artist has to change the posture of his hands dynamically such as rotating the calligraphy brush to perform certain strokes or dynamically changing forces to eroding wood while carving out wooden sculptures.

1.4 Research Question:

Can we use wearable sensors to extract the essence of human hand dexterity?

The human hand's ability to sense different objects should be learnt and should be studied by researchers. This tells us that we must try to extract the way human hand sense of touch is used to handle various objects. Studying the human hand's sense of touch and finding a way to quantify it should be the way to go ahead. There are various types of wearable sensors available today. Most of these sensors are used as bio-trackers which measure vital body data such as heart rate, blood oxygen levels etc. Normally these sensors are used to understand how humans burn calories during a workout. Similarly, to understand how humans use their sense of touch while handling different types of objects wearable tactile sensors can be used to study these aspects of object manipulation by human hands. Human in-hand manipulation involves not only object grasping but also moving the object within the workspace of the human hand by performing precise or fine motion. It must be noted that precise in-hand manipulation normally involves moving the object between fingertips on the human hand. Therefore, a wearable sensor which can measure tactile data around the fingertip area is required.

Hypothetically, we can employ wearable sensor to extract the essence of human hand dexterity. To extract the first essence of human hand dexterity we can use a wearable distributed 3-axis tactile sensor which can measure 3-axis force while manipulating the tool. To extract the second and third essence of human hand dexterity we can use the wearable exoskeleton or a data glove which can measure the position and orientation of the fingertips while handling the object. The dataglove should work in tandem with the wearble fingertip tactle sensors to measure the position of the fingertip tactile sensors while performing a manipulation task.

1.4.1 Purpose:

As mentioned earlier Japanese artisans are on the decline. Many young artisans normally are opting out of such manual and dying jobs. These artisans are skilled at various Japanese traditional crafts such as calligraphy, pottery, sculpting etc. There skills are a testament to the rich Japanese culture. It is necessary to safeguard this culture of Japan.

Let us take a small case of Ukiyo-e. Ukiyo-e used to be a a flourishing art style in contemporary Japan. Literature [1.9] studies the artists and print makers of the Ukiyo-e. A few Japanese wood printing artisans still exist today Once a flourishing industry is currently endangered. Many young artisans moving away from country side taking modern jobs endanger the survival of such traditional crafts. Fig1.11. shows a modern day ukiyo-e artists working on wood print arts.

Fig 1.11 Japanese Ukiyo-e artist working.

These artists take a lot of years to develop the art with gradual practice and training. It is necessary to safeguard such practices by the use of wearable sensors. With the help of wearable tactile sensors, we will be able to save these works of art in the form of the combination of tactile and position data. By doing so we can take the first step towards preservation of rich cultural heritage of Japan.

1.5 Connection with Robotics:

Collaborative robots or Co-bots have gained popularity in recent years. Many robots can be purchased and used as desktop robots. These robots can be expanded to accomplish applications in a plug-and-play manner. Collaborative robots can be employed to complete tasks that humans find manually repetitive and tiring. This functionality encourages small and medium-sized enterprises (SMEs) to incorporate this technology and continuously improve the operational efficiency of their workplace. Given their ease of use, modular design and flexibility in addressing variety of different tasks which can be performed with ease, many researchers including myself anticipate an increase in utilization of these types of desktop collaborative robots in recent years. These types of desktop collaborative robots have been utilized to work in environments in the close vicinity of human beings recently. However, normally these robots are utilized to perform mundane tasks such as pick and place tasks, object segregation tasks, etc. In the case of performing tasks that are more abstract and human-like the end effectors of these robots should have superior agility and strength. Also, the robot end effectors should have better dexterity similar to human hands. Nowadays the robot hands or end effectors should incorporate the use of precise tactile sensors which would give them the ability to handle objects of varying stiffness and shape in the physical environment. Different types of tactile sensors are used to sense objects while performing manipulation tasks. However even though the robot grippers have such capability the task performed by these grippers are limited to grasping different objects rather than manipulating moving different objects within the end effector framework. Human hand object manipulation involves not only on the grasping but also on moving the object within the workspace of the human hand. Therefore, robot end effectors should be reinforced with such capabilities. In order to enable robots to effectively work along side human workers we need to determine how robots will be able to assist humans by utilizing their robot end effectors to perform human like manipulations.

1.6 Research Objective:

The goal of this research is to create a combined 3 axis force and position sensing solution for extracting the essence of human hand dexterity. It is also necessary for the force and position sensing solution to be practical in its application. It is necessary to address multi-modalities such as distributed force sensing to address the requirement of measuring distributed 3-axis force over entire area of the fingertip. Also, it is required to increase the scope of the tactile sensor such that it is not just used for measuring tactile forces on the human hand but also be able to be attached on the robot hand as a robot hand fingertip.

1.7 Novel Contribution:

As mentioned previously, object interaction is not just limited to grasping applications, however it also involves manipulation of objects inside the human hand workspace. For example, during calligraphy the artist not only grasps the brush but also moves it dynamically to create strokes on the calligraphy paper. In this thesis we illustrate the design and development of “FingerTac” a wearable tactile sensor which can provide distributed 3 axis measurement around the area of the fingertip. The FingerTac sensor is designed such that it can be used as a fingertip of an Allegro-Hand as well making it the only sensor which can be worn by humans as well as robots. Further in this thesis we design and develop “ExoGlove” which when combined with the FingerTac can measure the position and orientation of the FingerTac while manipulating an object within the human hand workspace. This is the only available solution which provides a combined distributed 3 axis tactile measurement over the fingertip area along with measuring the position of the FingerTac. This will give us a rich information of the interaction forces.

1.8 Thesis Outline:

This section illustrates the synopsis of each chapter in this doctoral thesis. It gives the outline of the thesis at a glance.

1.8.1 Chapter 1: Introduction

This section is the introduction of the doctoral thesis. We explain the background. Importance of dexterity. This section explains the essence of dexterity and poses a research question asking the audience how we can extract the essence of dexterity using wearable sensors. Also, this sections describes the purpose of this research along with the research objective. Lastly it states the novel contribution of the research.

1.8.2 Chapter 2: Related works

This section illustrates the current related works of the existing wearable tactile sensors. These sensors are mostly single axis single sensing point sensors. This section also describes currently available multi sensing point single axis tactile sensing solutions. Further it describes the few 3-axis sensing solutions. They are an important reference and inspiration to design future wearable tactile sensors. Further it describes the novel or unexplored research area and also explains how the current research contributions of this thesis are novel to the currently available research.

1.8.3 Chapter 3: ExoGlove Version 1

This section illustrates the design and development of ExoGlove Version-1 along with the mechanical design of the Wearable Tactile Sensor Version-1. Wearable Tactile

Sensor Version-1 consists of a set of 4 compliant joints which are embedded with neodymium magnet each. These joints are placed around the finger pad area. Once the user manipulates the object the finger pad deforms displacing the magnet away from the center of the Hall-effect sensor. Raw data can further be calibrated to 3-axis force.
This section describes the problems encountered with the working of the sensor and illustrates how these problems can be tackled using the design of an Exoskeleton. Further this section presents the design of the ExoGlove version 1 which is used to measure the joint angles between finger segments while acting as a mechanical frame of reference to the sensors. Fig.1.12 illustrates the ExoGlove Version 1.

Fig 1.12 ExoGlove Version 1

1.8.4 Chapter 4: FingerTac

This section describes the design and development of the FingerTac. It describes the concept and its inspiration from existing work. It describes the working principle of the FingerTac and also describes the entire development and design process of the sensor. It

highlisghts its unique design features such as integration of the sensr with the robot hand called Allegro-Hand. This section describes the functional system design of the sensor. It also illustrates the process used for calibration of the sensor. Lastly it discusses the various application where this sensor can be applied.

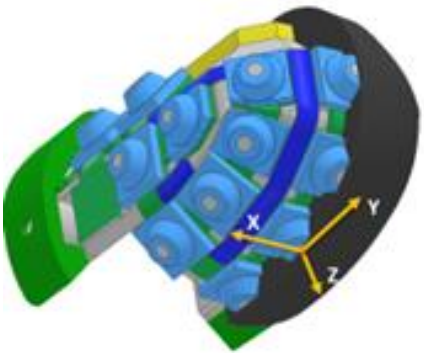

Fig 1.13 FingerTac - 3-axis distributed wearable Tactile sensor.

1.8.5 Chapter 5: ExoGlove Version 2

This section describes the design and development of the ExoGlove Version 2. It describes the concept and its inspiration from existing work. It also describe its mechanism used for the ExoGlove. It highlights the unique design features and the development and design of the encoder. It highlights the integration of the encoder within the revolute joints of the mechanism. It illustrates how the FingerTac can be integrated with the ExoGlove. Furthermore, it illustrates the functional system design of the FingerTac. It highlights the calibration of the ExoGlove encoder. It also describes the algorithm used for the calibration and also describes the algorithm used for forward kinematics of the ExoGlove. This section also illustrates the visualization program used to visualize the ExoGlove Version 2. Lastly this section presents the discussion about various application where this sensor can be applied.

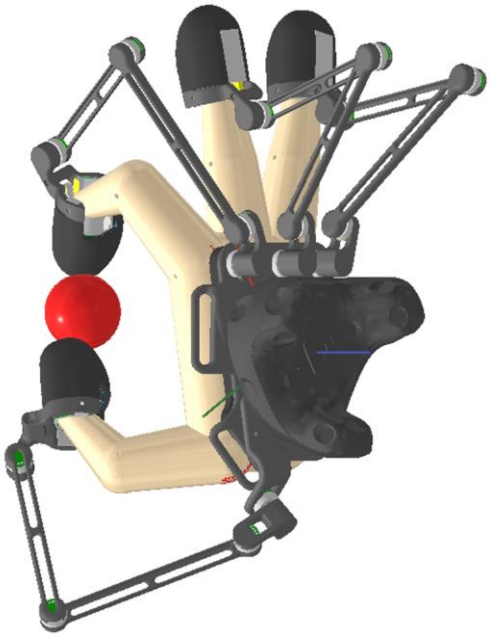

Fig 1.14 ExoGlove Version 2

1.8.6 Chapter 6: Future Works and Conclusion

This section describes the future works of the ExoGlove Version 2. This section presents how the ExoGlove Version 2 can be used as a device to map the human hand synergies to the synergies of the Allegro-Hand. This section also highlights the list of future works of the FingerTac.

Chapter 2

Related works

2.1 Introduction:

There have been multiple solutions which have been developed for measuring fingertip tactile force exerted by the human fingertip over the object. Overall, these solutions can be divided into the following sub categories:

1. **Single Axis Single sensing point:**
   As the name suggests these sensors are a single axis single sensing point sensors meaning that they can only measure force in Normal Axis or Z axis.

2. **Single Axis Multiple sensing point:**
   These sensors are generally in form of a glove which have distributed single axis sensing points over the palmar side of the fingertip area. They can only measure force in Z axis.

3. **Tri Axis Single sensing point:**
   These sensors are generally rare but are a supplement to the existing wearable tactile sensing solutions. These sensors can detect 3-axis force at a single sensing point. These sensors are useful at detecting slip as well as normal forces.

4. Tri Axis Multiple sensing point (Novel research area):

This is an unexplored research area as Tri Axis multiple sensing point solution is not available. Therefore, this is a novel research area. This doctoral thesis focusses on making contributions in this realm. This thesis describes the development of FingerTac in chapter 4 which is the only sensing solutions which is able to measure 3-axis force distributed over multiple points. This is a novel contribution to the field of wearable tactile sensing.

Let us go over the above subcategories one by one and describe the various tactile sensors currently available which belong to these subcategories.

In summary the current available categories can be arranged in the wearable tactile sensor canvass as shown in the Fig 2.1.

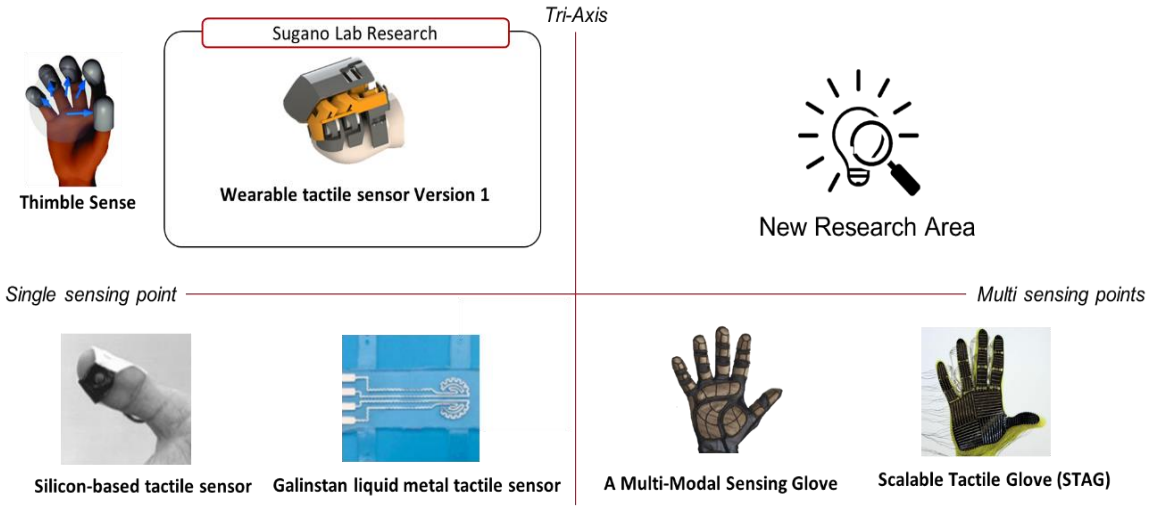

Fig 2.1 Wearable Tactile Sensor Canvass

2.2 Single Axis Single Sensing Point Solutions:

The wearable device consisted of a single piezo-resistive tactile sensor as shown in the literature [2.1] wrapped around the fingertip as shown in the Fig 2.2 To safely distribute the force applied on the sensor while handling an object, a dome was designed which covered the top surface of the sensor.

Even though the concept of a wearable tactile sensor was innovative, the sensor comprised of only a single taxel which covered most of the contact area on the palmar side of the fingertip. One of the limitations of the sensor was that it could only measure normal force.

Also the mechanical form factor of the sensor prevented the sensor from being distributed over different areas around the fingertip. This limited the potential of the sensor to be used in measuring tactile forces generated while performing grasping tasks only.

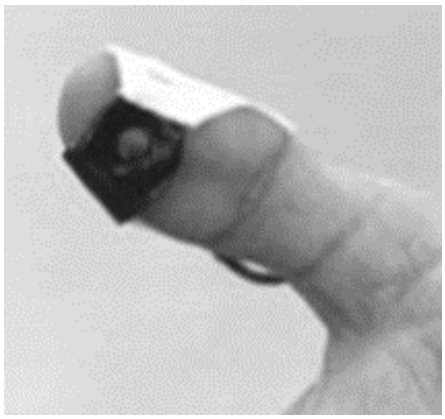

Fig 2.2 Silicon-based Tactile sensor

A wearable tactile sensor was introduced by [2.2]. The sensor consists of a piezoelectric material called PDMS and is worn on the user's palmar side of the fingertip. When the PDMS structure is mechanically deformed due to external force,

electric charges are generated within the material.

The generated values of the charges were calibrated to measure force by using a neural network. Although the authors claim to have good results at measuring forces accurately, it must be noted that the sensor is bulky in construction and as a whole function as a single sensing point. Also, due to the large form factor of the sensor, it cannot be distributed over the entire surface of the fingertip. This again limits the potential of the sensor to be used while performing grasping tasks only.

An interesting use case of liquid metal to be used as a tactile sensor was presented in literature [2.3]. Along with tactile information the sensor is also able to measure temperature. The sensor is made by sandwiching Galinstan liquid between two layers of PDMS material and can act as a tactile sensor to measure force in the normal direction.

The material can withstand high degrees of bending and stretching. However, it should be noted that the form factor of the sensor limits this sensor to be distributed over the entire surface of the fingertip. Also, as mentioned previously, human object handling relies not only on normal force but also on shear force, thus limits the use of these devices to quantify a holistic view of object handling and grasping.

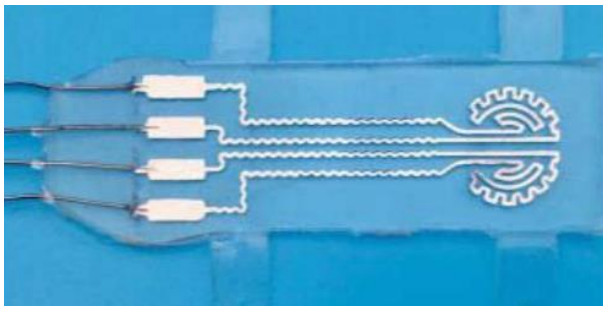

Fig 2.3 Galinstan Liquid based wearable Tactile sensor

Generally the single axis single sensing point solutions are widely available. They are the most researched sensor systems some of the notable ones include a wearable knit type tactile sensors[2.4]

2.3 Single Axis Multi Sensing Point Solutions:

Wearable multi-modal sensing glove was presented in literature [2.5]. The sensors embedded in the glove measure the pressure acting on the different parts of the hand. The tactile sensor used is a piezo resistive fabric sensor which is spread across various parts of the finger to measure tactile forces.

Along with the tactile information the wearable device also measures hand pose while performing grasping tasks on various objects. The distributed tactile sensing glove can be seen in the Fig 2.4

Fig 2.4 Multi modal tactile sensing glove

A wearable tactile glove is presented by [2.6]. The glove features 584 closely knitted sensors distributed across the entire hand as shown in the Fig 2.5. The sensors use piezo resistance as their working principle and are used to measure normal force only. The authors claim to have higher accuracy for heavier objects.

Accuracy of measuring force lowers as the weight of the object decreases. This implies that the glove might not be a favorable option to use for measuring forces which are present in fine manipulation tasks.

Fig 2.5 Scalable Tactile Glove (STAG)

2.4 Tri Axis Single Sensing Point Solutions:

[2.7] [2.8] presented ThimbleSense, a wearable tactile force sensor which is manufactured by embedding industrial grade force-torque sensors. The concept of thimble sense can be seen in the Fig. 2.6. In both devices, the force-torque sensors were encapsulated within a cap-like structure which is meant to be worn on the finger while manipulating an object. The paper suggests that the purpose of developing such a device was to measure accurate tactile force measurement and study sensorimotor control during grasps and manipulation while applying forces and manipulating an object. Though this method could accurately measure forces while manipulating different objects, the mechanical design of this sensor is not anthropomorphic in nature. Only a single force-torque sensor is used, and therefore only one force vector per fingertip could be obtained, albeit including also torques.

Fig 2.6 Thimble sense (STAG)

In the past our lab developed a series of unobtrusive tactile sensors for measuring shear and normal forces applied on the human fingertips while handling objects as illustrated in the manuscripts [2.9], [2.10], [2.11], [2.12]. Although, the latest iteration of the sensor [2.12] as shown in the Fig 2.7 provided good results and was effective at measuring normal and shear forces, the sensor functioned as a single sensing point

tactile sensor.

Thus the sensor was incapable of acquiring distributed force over the entire surface of the fingertip. Also, the lever design which is illustrated mechanically limits the user from performing tasks with the sides of the fingertips.

Fig 2.7 Wearable tactile sensor for human fingertips (Sugano Lab research)

The above sensor uses the fingerpad deformation principle to measure tactile force. s of The human fingertip pulp Characteristic were highlighted in [2.13]. They produce experiments with 20 subjects to study the finger pulp. The research suggestes that due to the effect of the external normal load on the human skin of the fingertip, the fingertip pulp stretches horizontally in response. Research has also gone towards creating a structural model of the finger pulp [2.14]. The research proves that the skin has similar behavior to the viscosity of the silicone material. We can see that research has been conducted to study deformation of the skin in normal force however deformation in the shear force is rarely been studied [2.15]. Finger flesh deformation in non linear manner has been simulated as [2.16]. Overall there has been research on wearbale tactile solutions which measure forces on the fngerpad, one of the pioneering research was conducted by [2.17].

There are some of notable wearable unobtrusive tactile sensors such as

Chapter 3

ExoGlove Version 1

3.1 Introduction:

To embark on the journey to have a combined 3 axis tactile force and position sensing solution for extracting human hand dexterity, I started by examining the shortcoming of the currently available wearable tactile sensors in Sugano Lab. As mentioned earlier I had worked extensively on the design and development of unobtrusive wearable 3-axis tactile sensors as presented in the literature [2.8], [2.9].

During the final year of my master's program at Waseda I had worked on [2.10]. These sensors are effective at measuring 3-axis forces. The sensor presented in [2.10] comprised of compliant mechanical joints placed around the fingertip area. Furthermore, I worked on the mechanical design of this sensor and while transitioning towards the PhD I published a RSJ paper [3.1].

The wearable tactile sensor provided a 3-axis tactile measurement of interaction forces while manipulating an object. Hence to have a combined position as well as tactile force measurement, an ExoGlove was designed. The ExoGlove functioned as a dual purpose device. It was able to measure the joint angle between finger segments while improving the functionality of the Wearable Tactile sensor.

Artists use most of the tools between the fingertips. The fingertips are used to manipulate the tool to generate fine manipulation tasks. Hence we will be showcasing how the functional performance of the wearable tactile sensors for fingertips is improved by the ExoGlove.

3.2 Mechanical design of the ExoGlove:

This section describes the mechanical design of ExoGlove. The ExoGlove consists of remote center of motion mechanism between every finger segment. The remote center of motion mechanism comprises of 6 linkages. Arranged in a specific manner to allow the linkages to rotate about the remote center of motion. Such linkages are widely used in surgical devices where the tool needs to rotate about a center of rotation which is inaccessible to the doctor. A lot of prior research has been conducted on RCM mechanisms [3.2], [3.3]. Many of the surgical robots also use RCM mechanisms [3.4],[3.5]. Meanwhile, RCM mechanism have been studied extensively such that it can be modelled kinematcally as presented in the literature[3.6]

3.2.1 Human finger Kinematics:

The human hand finger joint kinematics has been mentioned in the literature [3.7] consists of four revolute pairs and three joints. The one degree of freedom joints is namely, DIP (Distal Interphalangeal) joint and PIP (Proximal interphalangeal) joint as shown in the Fig 3.1. The MCP (Metacarpal Interphalangeal) is a two degree of freedom joint as shown in the Fig 3.1. Overall, the human finger comprises of four degrees of freedom. To measure the joint angles at these locations we will have to place the encoders at the other side of the finger which can increase the overall dimension of ExoGlove. Hence one way to measure the joint angle is through an indirect approach of Remote Center of Motion mechanism. This mechanism can be designed such that it rotates remotely at the center of one of the freedom revolute joints.

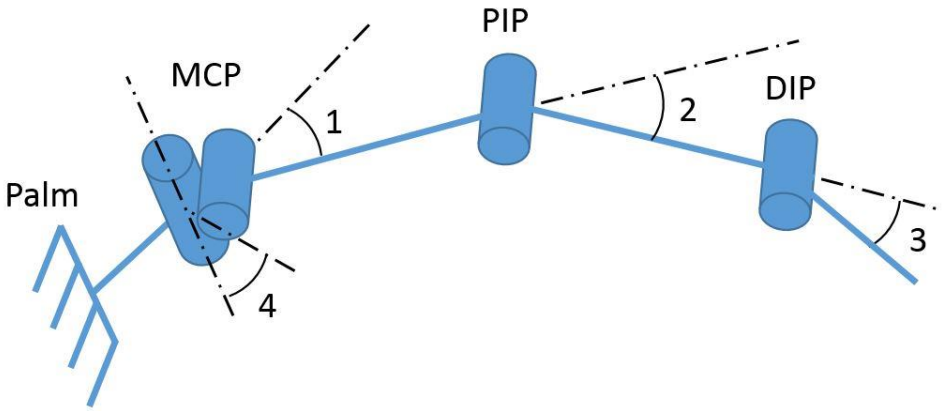

Fig 3.1. Human Finger kinematics

3.2.2 Remote center of Motion mechanism:

Previously in our lab we have used and studied Remote center of motion mechanism as presented in the literature [3.8],[3.9]. The following figure depicts the ExoGlove concept with the Remote Center of Motion (RCM) Mechanism. It consists of six linkages arranged parallelly. The remote center of rotation is kept at the center of the finger joints. The remote center is represented as T as shown in the Fig 3.2 and Fig 3.3.

The remote center T is aligned with the center of the finger by adjusting the angles 1 and 2. It should be noted that Linkages DE and AB are parallel and equal in lengths. Similarly linkage CD and AF are equal length and arranged in parallel to one another. Linkage BE and FC are arranged such that their bisect at lengths which are equal to DE and AB and CD and AF respectively. Thus it should be noted that CDEG and ABGF both act as parallelograms.

During the motion of the finger while flexing the DIP joint in this case, the link AF moves in sync with the wearable tactile sensor allowing the linkage to operate in such a way that the wearable tactile sensor rotates about the center of the DIP joint. This allows the sensor to move in sync with the fingers while the linkage functions as a mechanical frame of reference. Each revolute joint of the RCM mechanism houses a bearing to allow for frictionless motion while moving in sync with the user's hands.

Similarly, the links for the RCM mechanism were designed over the joints PIP and MCP. To address the MCP joint's second degree of freedom a simple revolute joint was designed. The RCM mechanism were designed to connect to a harness worn by the user on the palm. This functioned as a fixed frame of reference for ExoGlove. The palm harness was designed to be attached to the users arm with the help of elastic straps.

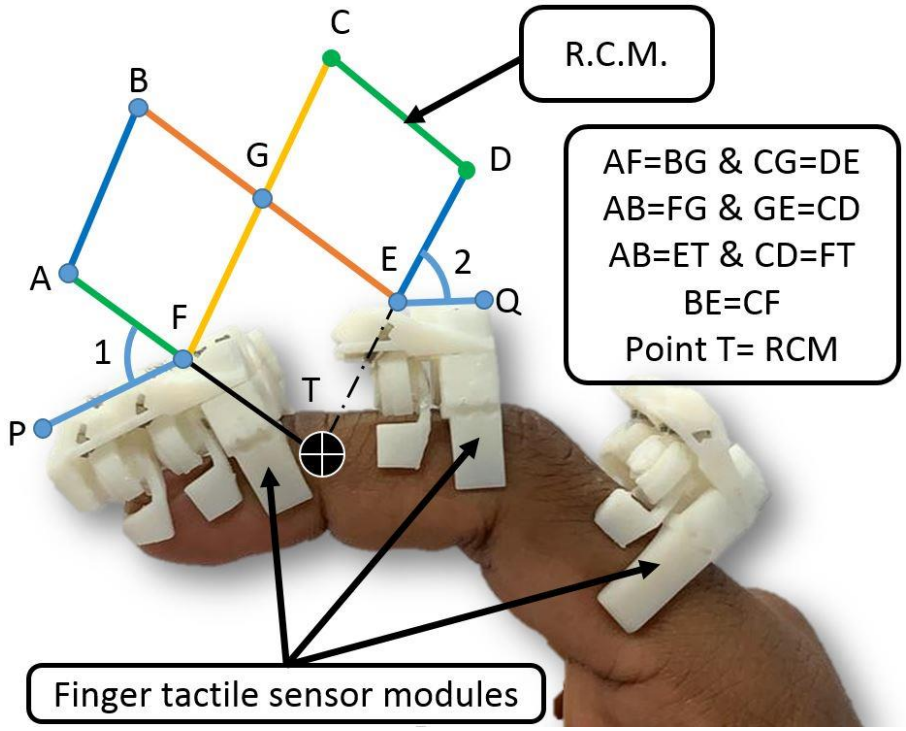

Fig 3.2. RCM mechanism kinematic before Flexing

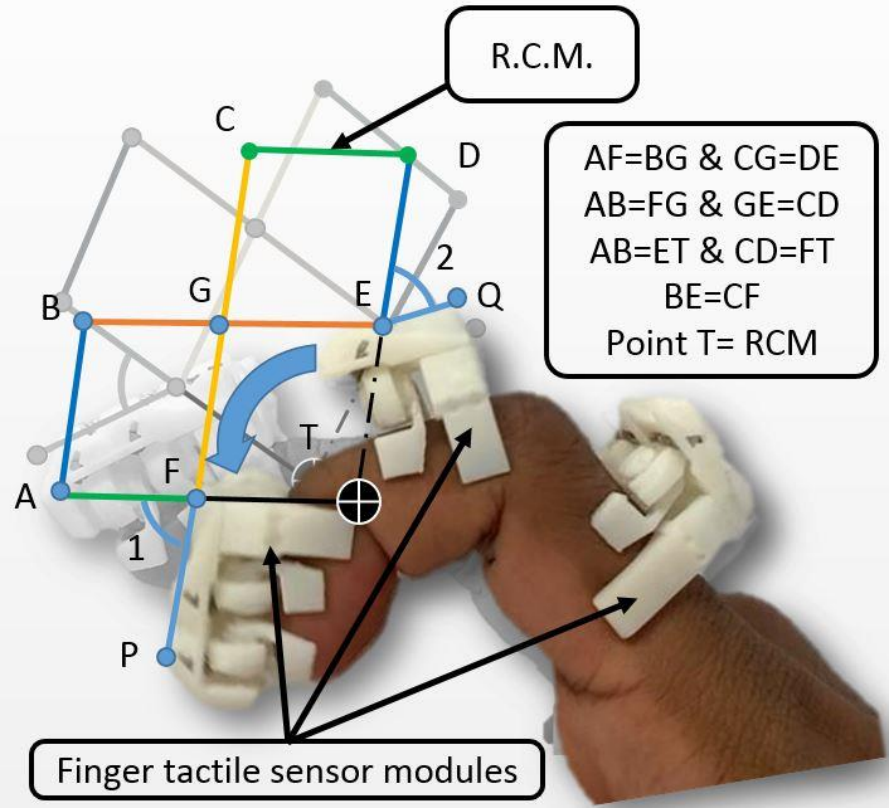

Fig 3.3. RCM mechanism kinematic after Flexing

3.2.3 Joint Encoder Design:

To fulfill the requirement of combined position sensing along with 3-axis tactile sensing, a hall effect based joint encoder was designed and placed within the revolute joint of two mechanical linkages. Fig 3.2 shows the Exploded view of the Hall-Effect based Encoder. The MLX90393 is used as the sensor through which the joint measurement can be realized.

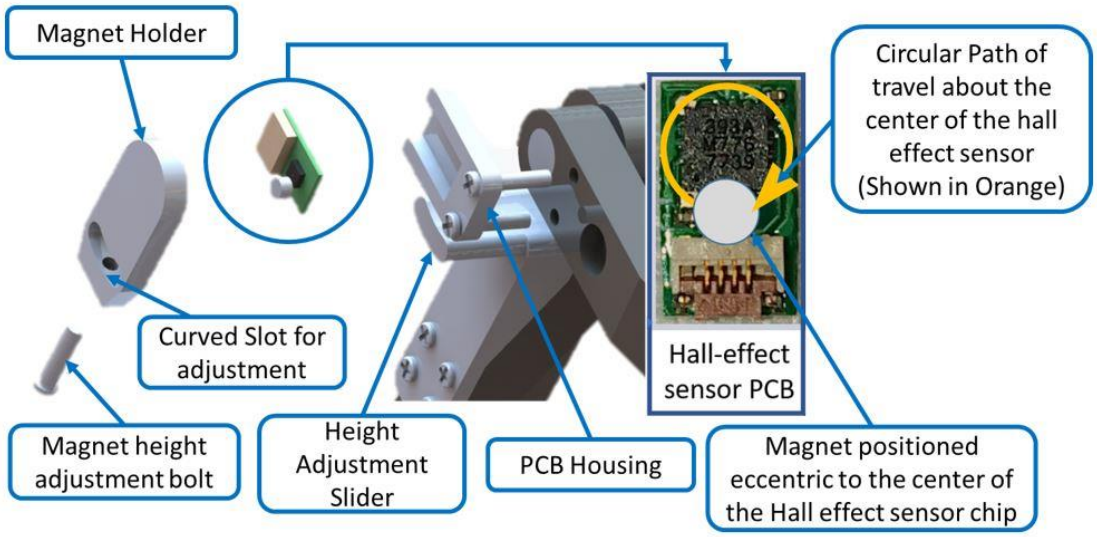

Fig 3.4 Exploded view of the Hall effect based Encoder.

The Hall-Effect sensor which is used to measure the joint angle is also used to measure the tactile interaction forces allowing the electronic system to be similar in function or operation to the Wearable Hall-Effect based Tactile sensors.

Previously eccentrically positions magnetic encoders have been researched before such as presented in the literature [3.10]. Similarly in our design, Encoder consists of a neodymium permanent magnet arranged eccentric to the center of the Hall-Effect sensor PCB. It is housed within a holder such that the north face of the magnet faces downward. The magnet holder is designed to be adjusted such that the user can change the height of the magnet over the Hall-Effect sensor PCB by sliding the magnet holder upwards or downwards.

The magnet holder is designed such that it can be loosened or fastened according to the user's needs. Fig 3.5 shows the encoder embedded in the ExoGlove measure the corresponding joint angles of the human finger joints (DIP, PIP, and MCP).

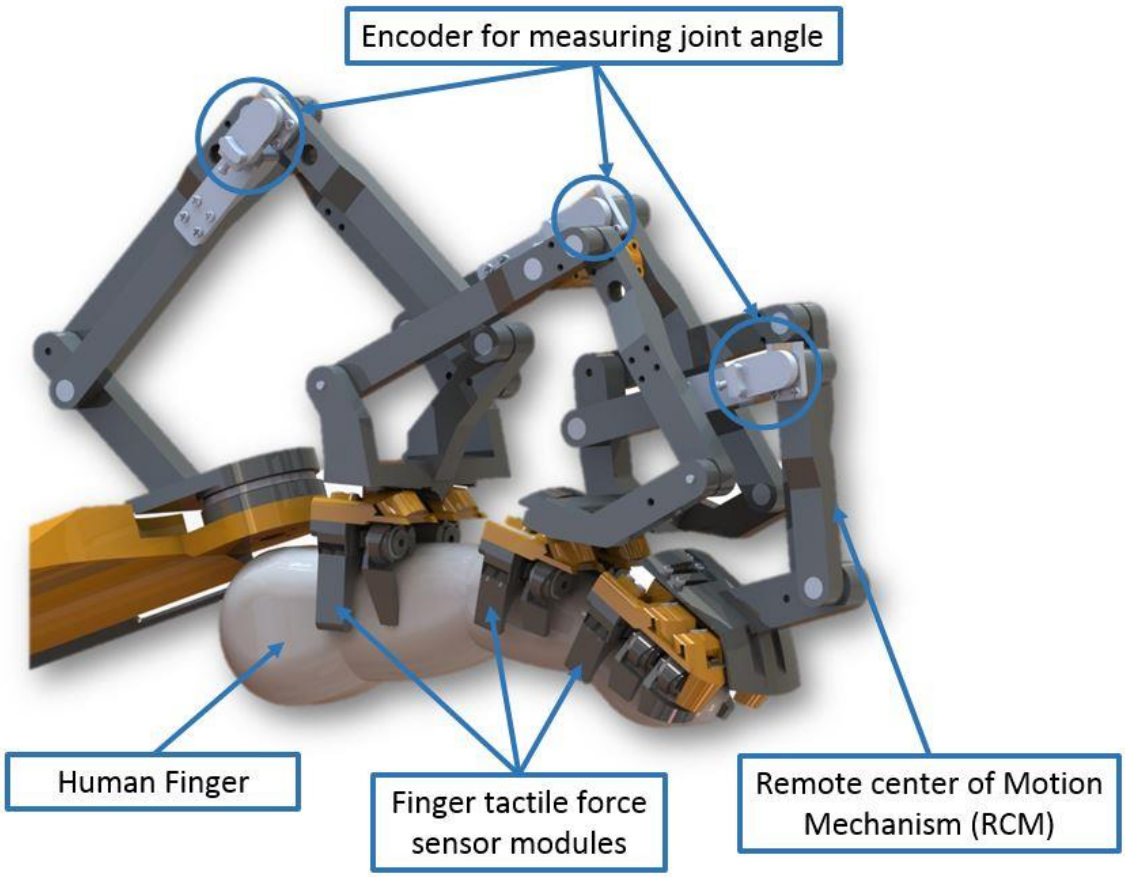

Fig 3.5 Encoder is embedded within the linkages of the ExoGlove.

3.3 Evaluation of ExoGlove Usage:

The ExoGlove is attached to the wearable fingertip tactile sensor using a 3D printed adapter which is manufactured using SLA based 3D printers. The sensors were attached with the adapters using a simple bolt and nut arrangement. The linkage mechanism was manufactured using an extrusion-based 3D printer with PLA material.

The ExoGlove was worn on top of the user's palm by using the elastic harness as shown in the figure. The user was asked to attach the sensors to the finger segments and the user was then asked to flex and extend the finger as shown in the Fig 3.6 and 3.7 below.

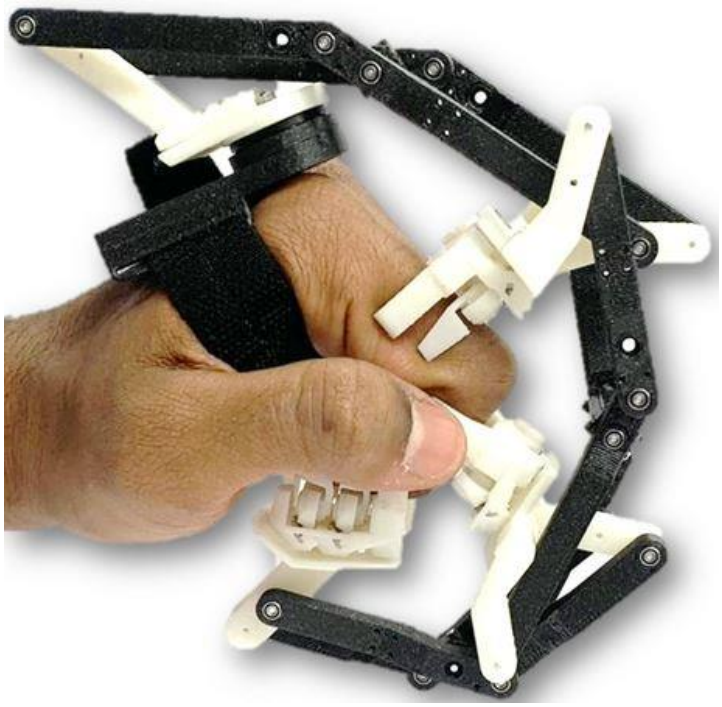

Fig 3.6 ExoGlove in Flexion.

Here we can see that the ExoGlove mechanism allows the user to flex the finegr however the flexion is partial as the user cannot completely close the fist. Eventhough there is a partial flexion the ExoGlove can be used to perfom different application which

do not require full flexion and extension.

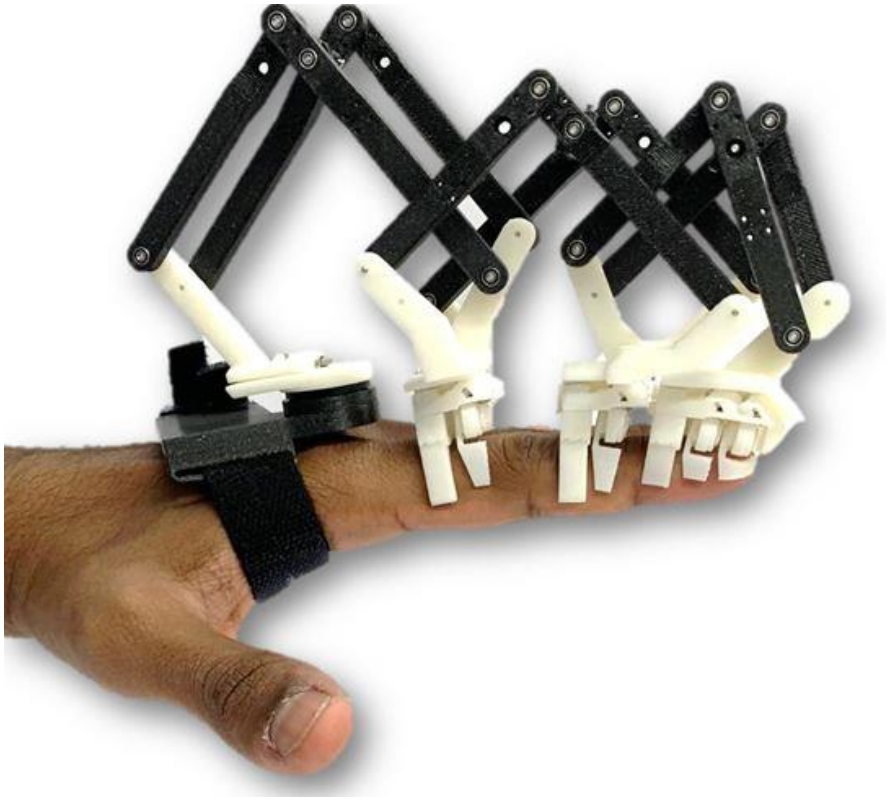

Fig 3.7 ExoGlove in Flexion.

It is evident from the above two figures that the ExoGlove is able to follow the wearable fingertip tactile sensors while allowing a non hindering motion through the manipulation process. It must be noted that non-hindrance is an important property of a wearable device and thus we are able to provide such synchronised motion using the ExoGlove.

Further the ExoGlove can be used to interact with different types of object. It should be noted that the ExoGlove is also equipped with the sensors at the finger segments meaning that it can be used effectively for grasping applications as well.

Fig 3.8 shows the ExoGlove interacting with different objects. It is evident from the figure that the user can interact with the object without any hinderance to the wearer's finger. The ExoGlove can be used in various types of grasps even mine manipulation

grasps such as pinch grasps.

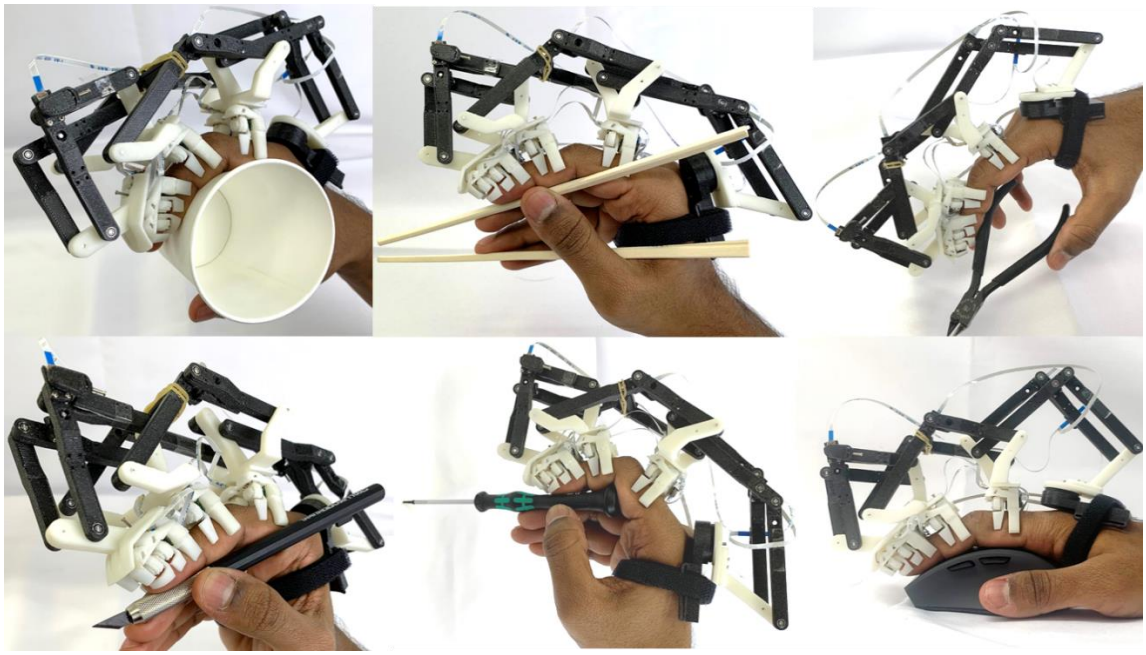

Fig 3.8 ExoGlove interacting with different objects

The ExoGlove can be used for fine grasps such as holding forceps or holding chopsticks. However, its usage in the field of hand manipulation is doubtful. As the finger segments have the compliant joint s situated around the fingertip and the finger segment area it is difficult to envision the usage of the ExoGlove in the field of in-hand manipulation of an object.

3.4 Evaluation of ExoGlove as a Dataglove:

It should be noted that the human finger joint does not have a rolling motion hence it is difficult to find the center of rotation of the finger joint. Even if it is a difficult task to locate the exact center of the joint angles of the DataGlove it is very difficult to calculate the exact joint angle of the finger joint. To solve this problem physicians normally use a Goniometer. The goniometer is a tool to measure the joint angle of the of the finger during flexion and extension. This literature uses a goniometer to form measuring angular movement[3.11]. Overall the goniometer This tool has been widely used by physiotherapists to check the range of motion of a particular joint in the human body. Therefore, to evaluate the ExoGlove encoder's ability to measure the joint angles we will be using a Goniometer as a Ground truth.

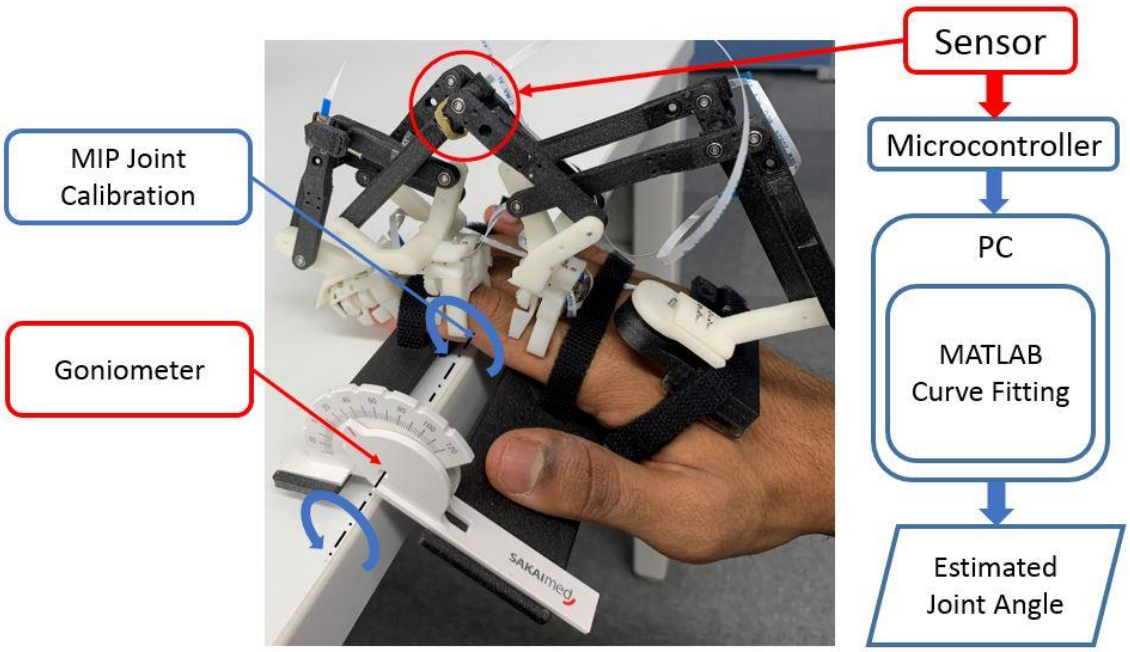

Fig 3.7 ExoGlove in Flexion.

The Goniometer was thus attached to the ExoGlove to calibrate the device by using a simple arrangement as shown in the Fig 3.9. One side of the Gonio meter was attached to the finger segments whereas the other side was attached to the palm of the user. The

user was then asked to wear the ExoGlove and was then asked to rest the middle and distal phalanges on the surface of the table. The user was then asked to slowly flex the PIP joint by performing sequential motions of 5 degrees. Every 5 degrees the Raw readings on the Encoder were noted against the actual angular measurements of the Goniometer.

A linear model was used to convert the raw measurements of the Hall-Effect based encoder and calibration parameters were calculated using MATLAB curve fitting using the Statistical and Machine learning toolbox. Following equation was used to calibrate the raw values:

$$\theta = aX + bY + cZ \qquad (3.1)$$

Here θ is the calibrated angle measure of encoder output. The raw magnetic measurements are given by the X, Y, Z variables. The a, b, and c are the calibration variables which were calculated using the MATLAB tools.

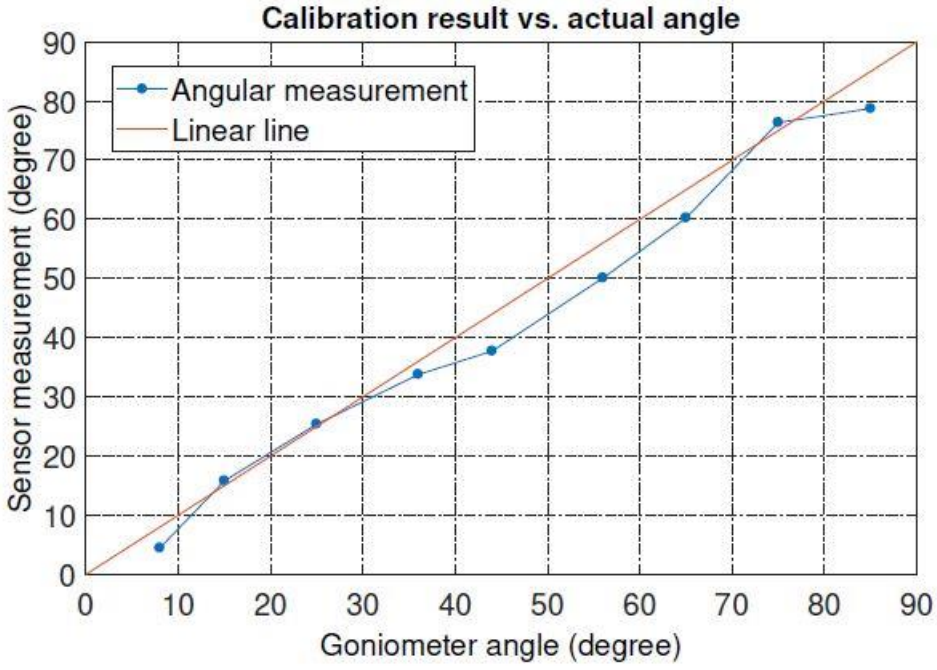

Fig 3.8 ExoGlove in Flexion.

To test the behavior of the encoder, the user was asked to flex the PIP joint with an increment of 10 degrees. The calibrated encoder measurements were compared with the actual measurements of the goniometer as shown in the Fig 3.8. The blue line shows the result of the from our proposed angular sensor vs the values from the goniometer. Overall, a variation of +/-5 degrees was observed in the encoder readings over the range of 90 degrees. From these results we can say that the sensor can be used for measuring angular measurements. ExoGlove along with the wearable tactile sensor for fingertips is able to work as a combined 3-axis and position sensing solution.

Chapter 4

FingerTac - Wearable Distributed 3-Axis Tactile Sensor:

4.1 Previous Research uSkin:

In Sugano Laboratory, we have developed a tactile sensor called uSkin as shown in the Fig 4.1 featured in the literature [4.1]. This tactile sensor is designed based on the Hall-effect sensing principle.

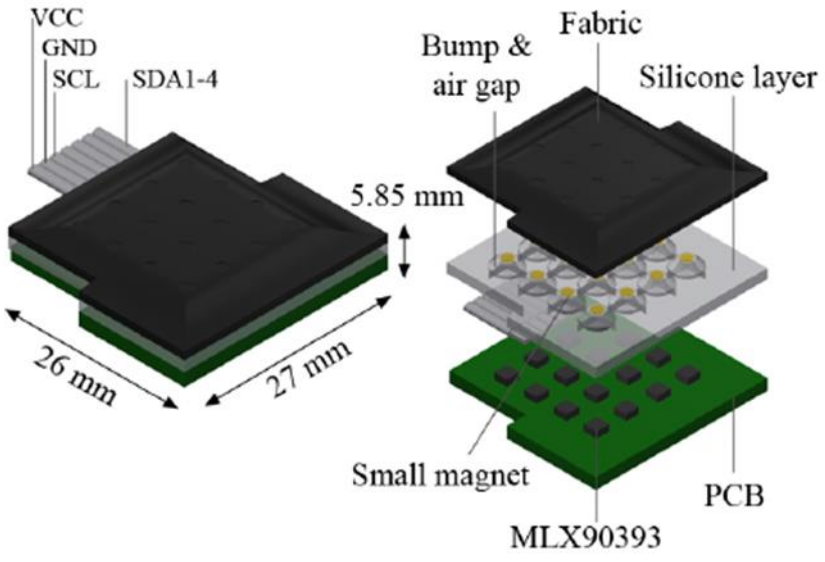

Fig 4.1 uSkin

4.1.1 Working Principle:

The uSkin consisted of a permanent magnet embedded within a silicone dome attached on top of a Hall-effect sensor. The change in the magnetic field in the vicinity of the Hall-effect sensor was detected by the Hall-effect sensor and was interpreted as tactile data.

The sensor has been developed further and has been implemented to cover the robot fingers phalanges as illustrated in the literature [4.2]. Also, the sensor has been developed previously to cover robot fingertips which are anthropomorphic in nature as illustrated in the literature [4.3].

4.1.2 Transition from Bulk Silicone Design:

Previous uSkin sensors had a continuous silicone skin layer embedded with multiple magnets. Therefore, displacement of one magnet resulted in the displacement of the adjacent magnet due to the presence of a continuous skin layer as described in the literature [4.1]. As a result, the adjacent hall effect sensors would also detect the change in magnetic field. This behavior is known as crosstalk. Hence, to alleviate crosstalk and improve the sensor response we have also experimented by optimizing the silicone skin structure to individual silicone dome structure as described in the literature [4.4].

4.1.3 Silicone Dome Design:

Currently, uSkin consists of an array of Hall-effect sensors arranged in a square or rectangular configuration. As shown in the Fig.4.1. The new silicone skin consisted of an array of silicone domes embedded with neodymium magnets. The new silicone skin is placed on top of the array of Hall-effect sensors as shown in the Fig.4.2 below. Under

the application of an external force Silicon Skin deforms displacing the magnet from its initial position in three-dimensional space. The silicone dome allows the permanent magnets to displace independently. The displacement of the magnet causes a change in the magnetic field around the vicinity of the Hall-effect sensor which can be detected by the Hall effect sensor. Each Hall effect sensor measures the change in the magnetic field as raw values in three axes X, Y, and Z. These raw values can be interpreted as tactile data. Going further the raw values can be calibrated to measure force by using a reference force torque sensor. Currently the Tactile sensor is also commercially available and can be manufactured for a customer specific application.

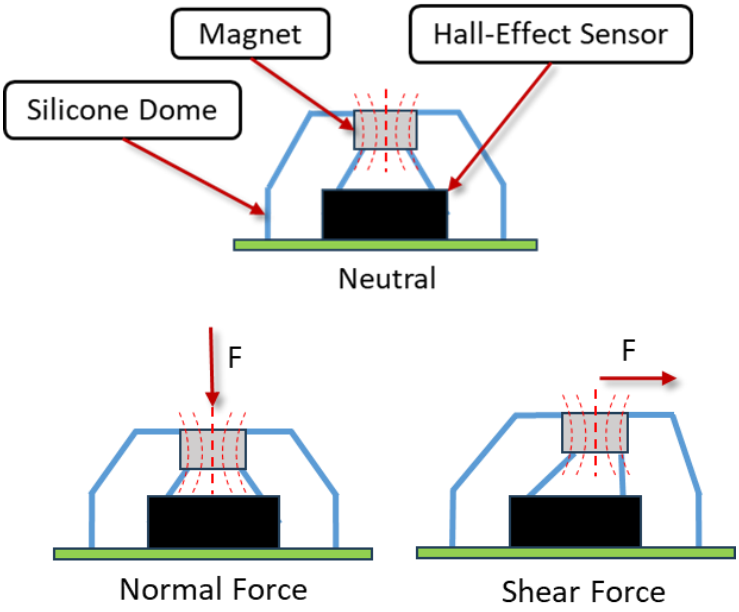

Fig 4.2 uSkin Silicone Dome Working Principle

4.2 Design of FingerTac:

Tactile skin sensors based on the Hall-effect principle are an effective and proven way to measure 3-axis force. Each dome design combined with the Hall-effect sensor of the uSkin can act as an individual three-axis sensing point which can provide tactile information. The uSkin dome design if combined with a flexible PCB can be modeled into various shapes or forms and thus in this case can be distributed over the entire surface of the fingertip of the human hand as well as the fingertip of the robot hand. This would increase the scope of the sensor to be used to measure tactile data in seemingly simple yet complex tasks such as rolling an object over the surface of the fingertip.

4.2.1 FingerTac Dome Design:

FingerTac sensor would be designed to be worn on the user's fingertips thereby forming a layer of sensing elements between the object and the fingertip. Even though the user won't be able to feel the object/tool under manipulation, it is required to provide the user with in-direct tactile sensation in order to manipulate the object effectively. This can be achieved by lowering the thickness of sensing elements between the fingertip and the object/tool. Thus, based on the uSkin dome design, a dome design for the FingerTac sensor was created as shown in the Fig.4.3 below.

The overall dimension of the dome design along with my PCB is 3x3x3mm (length x breadth x height). The form factor of the dome design is small and each dome design can function as a three axis independent tactile sensing points. These individual domes can be distributed over the fingertip surface thus giving the user the ability to sense and measure three axis data over the entire surface of the fingertip while handling objects/tools.

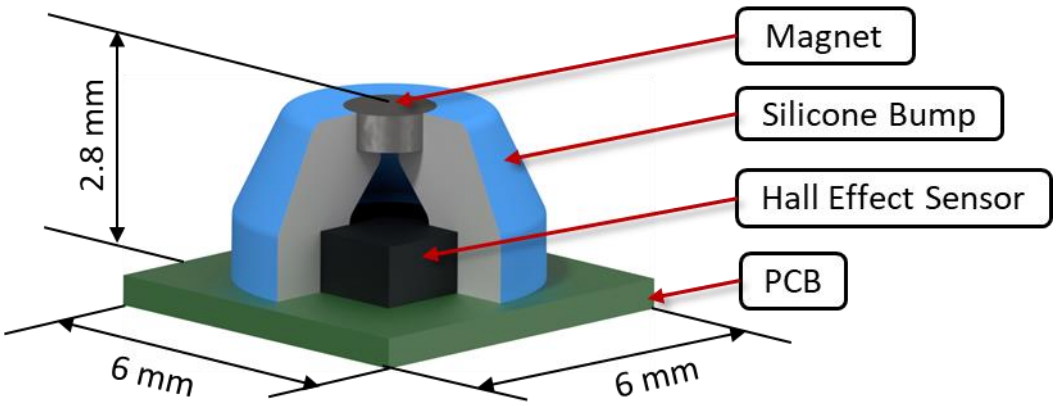

Fig 4.3 FingerTac Silicone Dome

4.2.2 Positioning of sensing points around the fingertip area:

It is necessary to first understand the most used area of the fingertip for grasping applications to position the sensing points. Literature [4.2] illustrates several areas of the fingertip which has been used for grasping applications. However, it must be noted that the new wearable tactile sensor is being designed not only for grasping applications but also for manipulation applications, especially applications that include fine manipulation tasks. This includes traversing objects being manipulated over several areas of the fingertips both thumb and fingertips.

To determine potential locations for tactile sensing points a small interactive study was conducted. Initially, a ping-pong ball was covered with white colored ink. The user was asked to wear a rubber finger sleeve as shown in the Fig.4.4a and was asked to hold the ping-pong ball between the fingertips in a two-point grasp as shown in Fig. 4.4a. The user was then asked to move the ping-pong ball naturally between the fingertips by performing slight movements as shown in Fig. 4.4b. Slight movements were made to traverse the ball

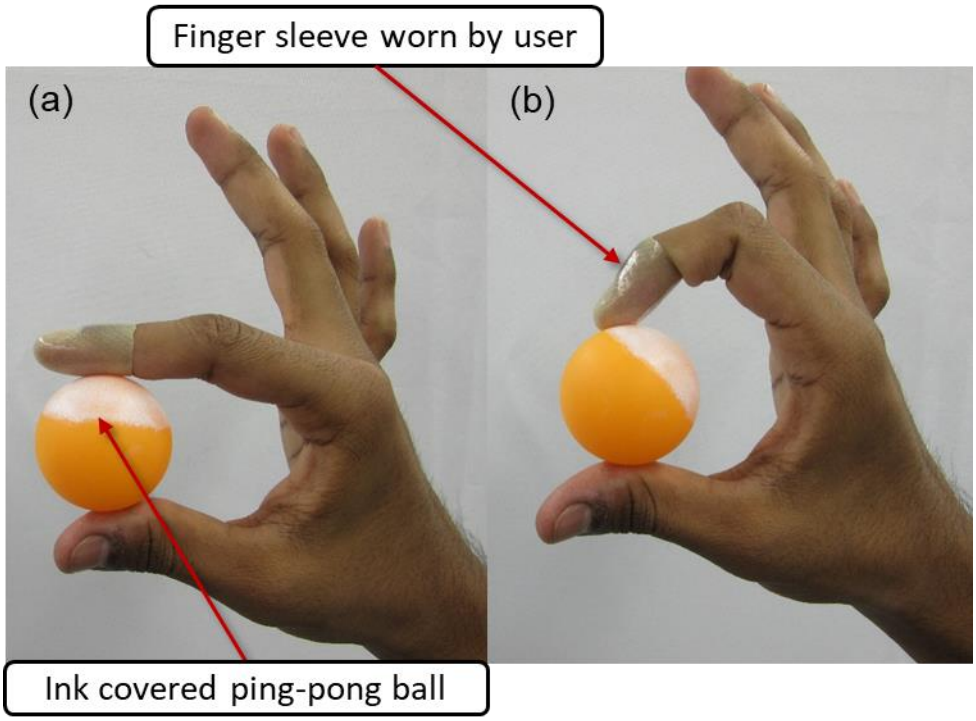

Fig 4.4 Interactive Study

around the fingertip area. As a result, the white colored ink was imprinted onto the user's fingertip. The imparted white-colored ink on the finger sleeve indicated the potential contact area between the ping-pong ball and the fingertips.

Using a minimum space of 5 mm between every sensing point, points were marked on the finger sleeve as shown in the Fig. 4.5. A CAD model of the finger sleeve was created. The CAD design resembled the finger sleeve as being worn on the fingertip of the user. The points marked on the finger sleeve were mapped onto the CAD model of the finger sleeve. The mapped points served as reference points for the positioning of the sensing points on the fingertip area.

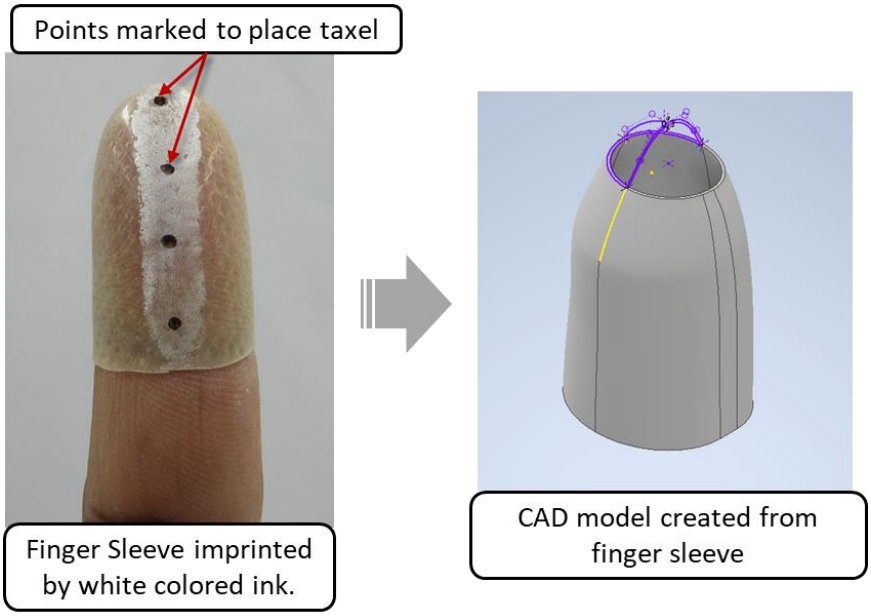

Fig 4.5 Finger sleeve CAD model

4.2.3 Designing the Homogeneous Rigid shell:

In order to provide a rigid mechanical reference point to the Hall-effect sensors a homogeneous rigid shell was necessary to be designed. Square-shaped rigid panels of size 5 mm by 5 mm were designed and placed at the points positioned around the finger sleeve.

The panels were connected to one another to create a homogenous rigid shell. The homogeneous shell was then 3D printed and checked to fit on the user's fingertip as shown in Fig 4.6.

It was evident that being a shell or cap-like structure it was susceptible to movement around the fingertip. To prevent this from happening a finger sleeve with a T-shaped slide on the top was designed and molded as shown in the Fig.4.7 below. To attach the newly molded finger sleeve to the homogeneous shell a slot was designed as shown in the Fig.4.7 below. The slot was designed to have enough tolerance to attach the sleeve and prevent the homogeneous shell from rotating around the fingertip area. Attention to

detail was given to the homogeneous shell by designing ridges to prevent the PCB layer from shifting laterally.

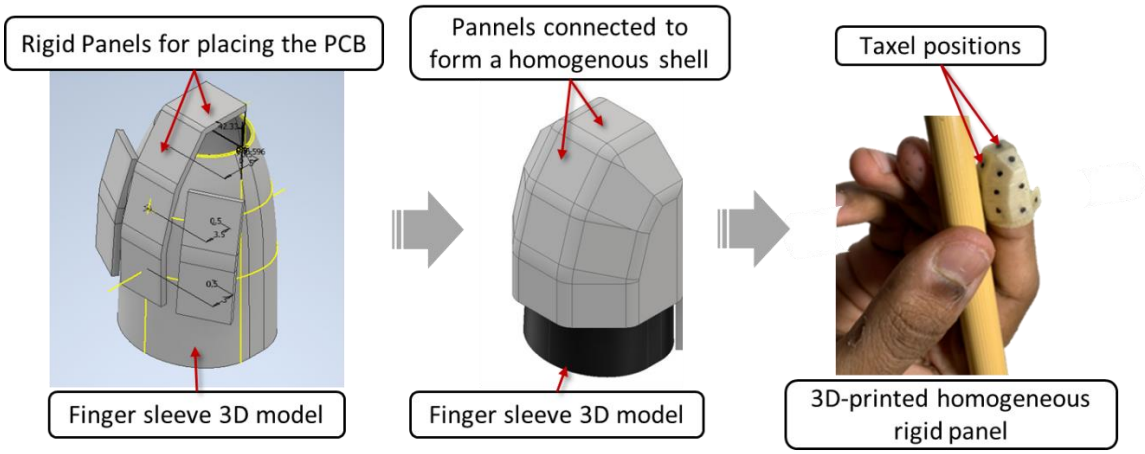

Fig 4.6 Finger sleeve CAD model

The homogeneous shell was 3D printed several times and through trial and error the final design was realized. The FingerTac was to be designed with a continuous outer skin layer. Hence to support the lateral side of the outer skin a special 3D printed collar was designed and attached on either side of the FingerTac homogenous rigid shell. The entire design was iterated many times before coming to a final design. The final design was printed using acrylic material using a 3D printer with laser sintering technology.

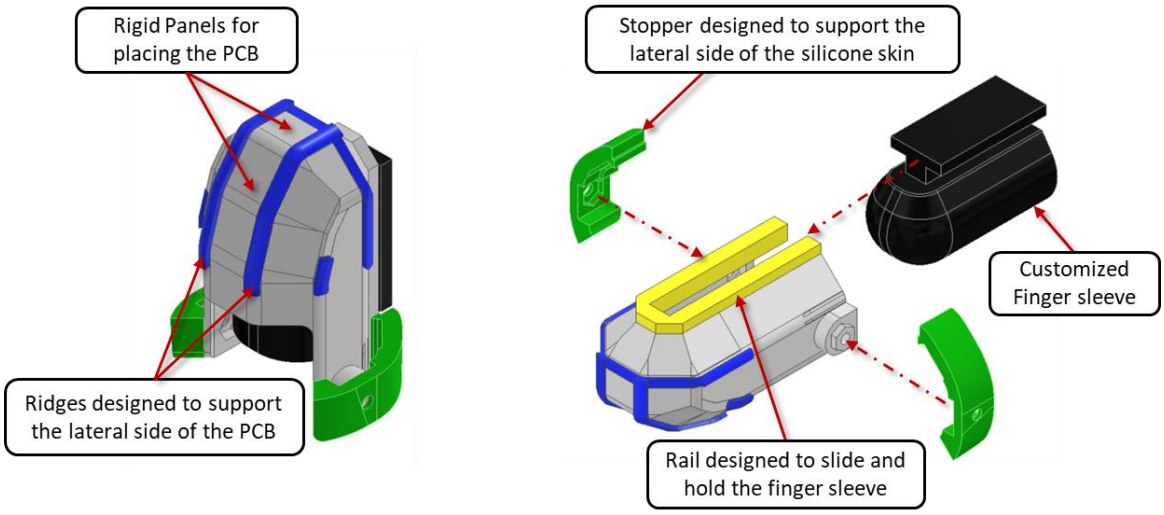

Fig 4.7 Homogeneous shell design

4.2.4 Designing the Flexible PCB:

The homogeneous rigid shell was used as a reference. A CAD design of the wrapped PCB around the homogenous rigid shell was designed as shown in the Fig.4.8 below. This design was created within the assembly of the homogenous shell.

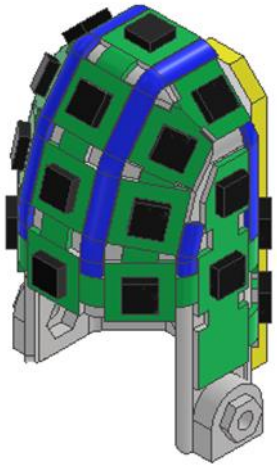

Fig 4.8 CAD design of Flexible PCB wrapped around homogenous shell

To reduce the thickness of the sensor the PCB thickness was kept as small as 0.6 mm Hall effect sensor IC was also designed and modeled in the CAD file. Using the CAD design unwrap tool, the PCB was unwrapped, and the outline of the unwrapped Flexible PCB was generated as shown in the Fig.4.8 below.

The outline of the PCB was edited and 90-degree corners were rounded off with smooth edges for ease of manufacturing. The unwrapped outline was converted into the DXF format and exported to the Autodesk EAGLE software. The outline served as the boundary of the flexible PCB. A schematic consisting of twenty Hall-effect sensor ICs routed using an I2C circuit was designed.

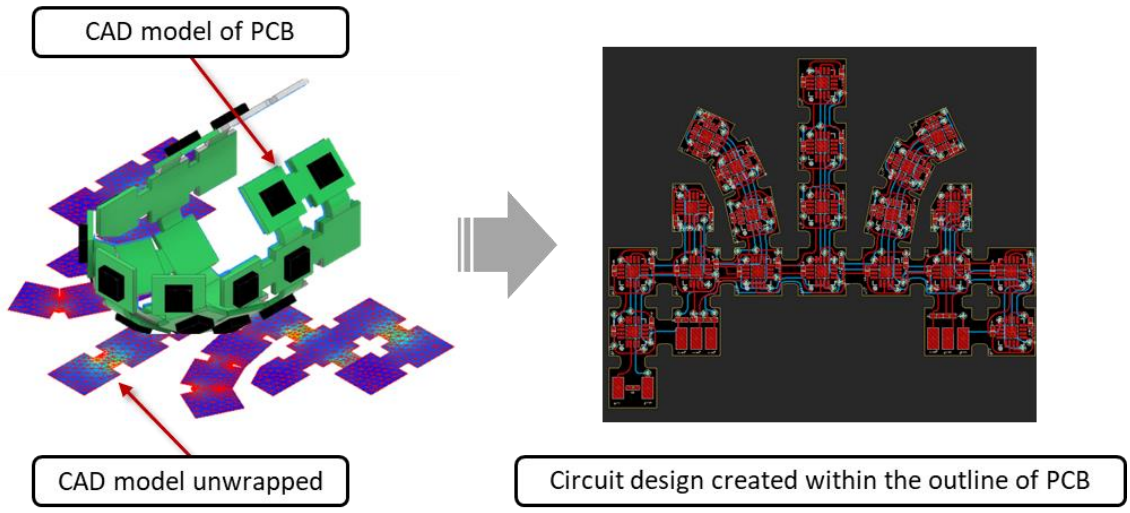

Fig 4.9 CAD design of Flexible PCB un- wrapped

The MLX90393 Hall-effect sensor from Melexis was chosen as the Hall-effect sensor. The MLX90393 is equipped with four I2C addresses namely, 00, 01, 10 and 11. To route the Hall-effect sensors, four ICs with different I2C addresses were combined together on the same data line (SDA line) using a daisy chain configuration. Therefore, in total there were five SDAs for one flexible PCB.

The Flexible PCB consisted of 3 layers. The first and second layers contained the actual routing of wires as shown in the Fig.4.10 below. The first two layers were manufactured using a flexible material.

The maximum bending of this material was up to 180 degrees. To support the soldered components such as the resisters, capacitors and the hall-effect sensor IC, it is necessary to apply a third layer to the flexible PCB as shown in the Fig. 4.10 below. This third layer acts as a hard layer or a stiffener layer. Overall PCB consists of flexible layers as well as hard layers as shown in the Fig.4.10 below.

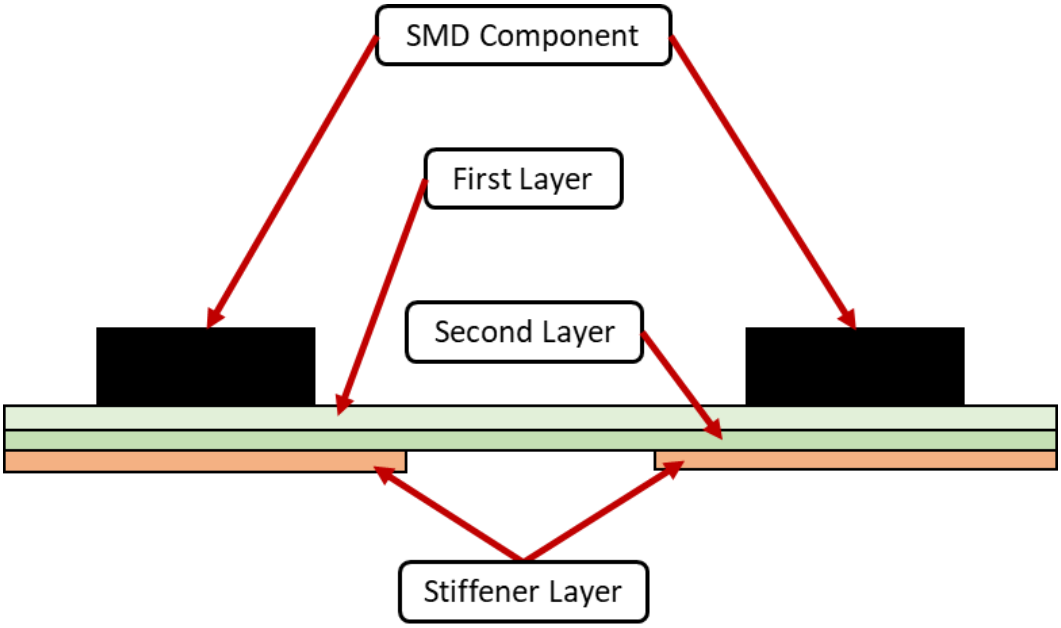

Fig 4.10 Structure of flexible PCB

4.2.5 Designing the Flexible dome skin and outer silicone skin:

The outline of the PCB used to design the boundary for the PCB layer was used to design the outline of the dome skin. To locate the center points of the Hall-effect sensor IPs, the center points of the square-shaped Hall-effect sensor ICs were marked on the outline generated by the PCB.

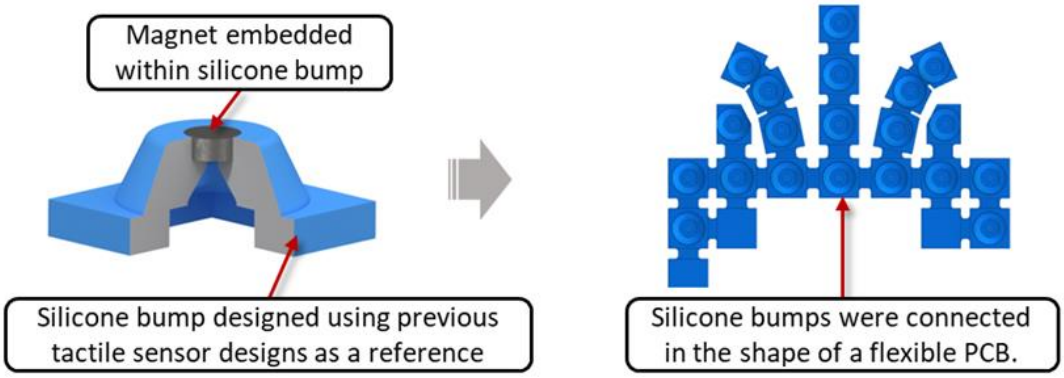

Fig 4.11 Structure of flexible PCB

These points served as the exact location of the Hall-effect sensor placement. The silicone domes were designed at these locations as shown in cross-section in the Fig..4.11

An overall thickness of 2.8 mm was maintained as the height of the domes while designing the dome skin. A two-part mold was created for the silicone dome skin as shown in the figure. An N50 neodymium magnet was chosen to be embedded in the silicone dome skin as shown in Fig 4.12.

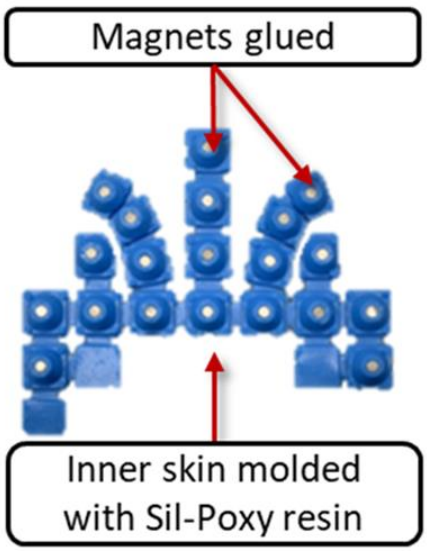

Fig 4.12 Silicone Dome Skin Embedded With Magnets

The silicone dome skin was then glued on to the flexible tactile sensor wrapped over the homogeneous shell shown in the Fig 4.13.

To have a continuous contact layer between the sensor and the object an extra layer of soft silicone was designed over the dome skin. A thickness of 0.5mm was maintained between the object and the top surface of the silicone skin. The thin thickness of the soft silicone layer over the dome design allows for a minimum thickness between the silicone dome and the object under manipulation.

The outer layer of the silicone layer also functioned as a protective layer for the magnets from external abrasion while manipulating the object as shown in the Fig 4.14.

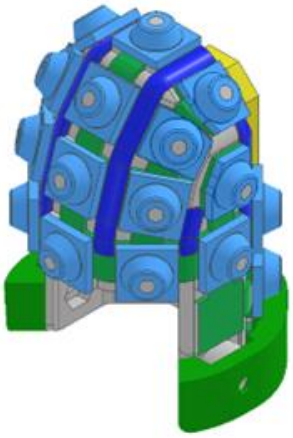

Fig 4.13 Silicone Dome Skin Molded Wrapped On The Homogeneous Shell

Overall, composite skin was realized with hard dome silicone skin underneath a soft silicone layer. A shore hardness of 00-50A was used to design the outer layer of silicone. Ecoflex 50 silicone rubber from smooth-on was used to mold the outer silicone skin. A shore hardness of 40A was used to design the inner dome silicone skin. SilPoxy is a hard silicone rubber which was used to mold the inner dome silicone skin.

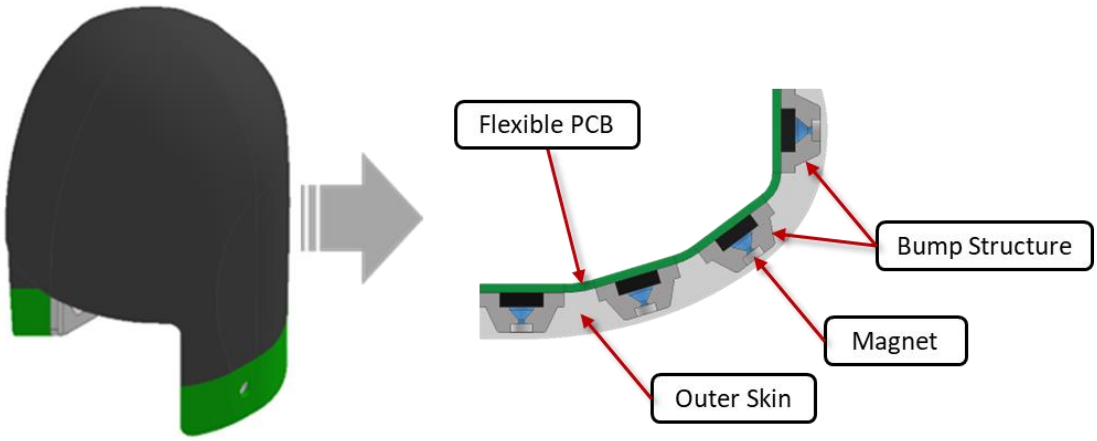

Fig 4.14 Outer Silicone Skin of FingerTac

4.3 The manufacturing process of FingerTac:

A comprehensive manufacturing process for manufacturing FingerTac is illustrated in this section. The process is simple to follow and the FingerTac is easy to manufacture.

4.3.1 Molding of the silicone dome structure:

Once the design of the silicone structure was completed, the next step involved is creating a mold for the precise shaping of the silicone. This mold was carefully crafted using two hollow blocks that would define the final form of the silicone structure. The use of two blocks allowed for the creation of a three-dimensional shape, ensuring an accurate representation of the intended design. (Refer Figure 4.15)

To introduce the silicone material into the mold, a rubber tube with a diameter of 5 mm was utilized. This tube served as a conduit for the liquid silicone, enabling it to be injected into the mold in a controlled manner.

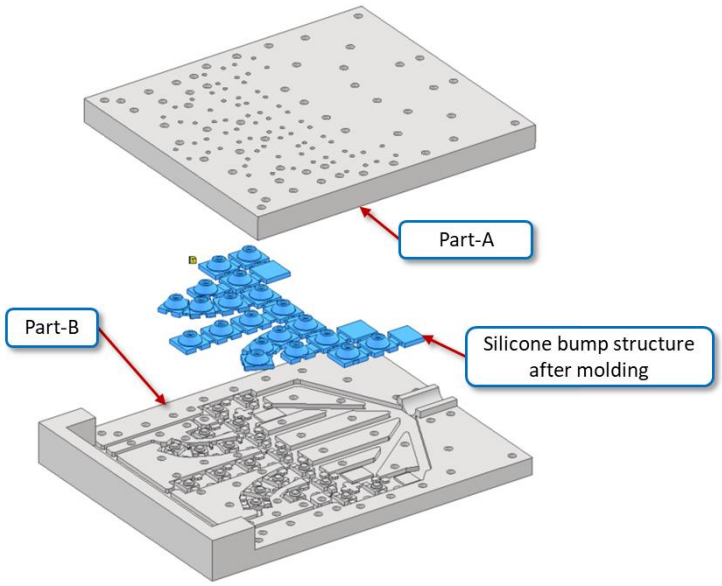

Fig 4.15 Slicone Dome skin Mold

A critical aspect of the molding process was the incorporation of a vacuum-assisted technique. This method involves using a vacuum to remove air and gases from the mold environment. By applying a vacuum during the molding process, any potential air bubbles within the liquid silicone were effectively eliminated. The vacuum-assisted molding process is crucial for achieving a bubble-free and uniform consistency in the final silicone structure.

In summary, the mold, designed with two hollow blocks, facilitated the shaping of the silicone, while the rubber tube and vacuum-assisted molding process ensured a precise, bubble-free outcome for the silicone skin. This meticulous approach is essential for maintaining the integrity and functionality of the silicone structure in the intended application.

4.3.2 Molding of composite silicone skin:

In a manner similar to the mold created for the silicone structure, three blocks—Part A, Part B, and Part C—were specifically designed to shape the outer skin layer. Fig.4.16 provides a visual representation of these blocks and their arrangement in the design. The three part mold was first assembled with the FingerTac embedded inside. The Ecoflex 50 was prepared in a container and was de-gassed to remove any air bubbles within the Ecoflex. A black colored silicone pigment was added to the Ecoflex which changed the color of the transparent silicone to a blackish color. This was done to improve the aesthetic appearance of the FingerTac. One end of a rubber hose was inserted inside the opening of the mold and the other end of the rubber hose was connected to a syringe. The syringe was filled with the Ecoflex material and a vacuum assisted molding technique was used to mold the outer skin of FingerTac.

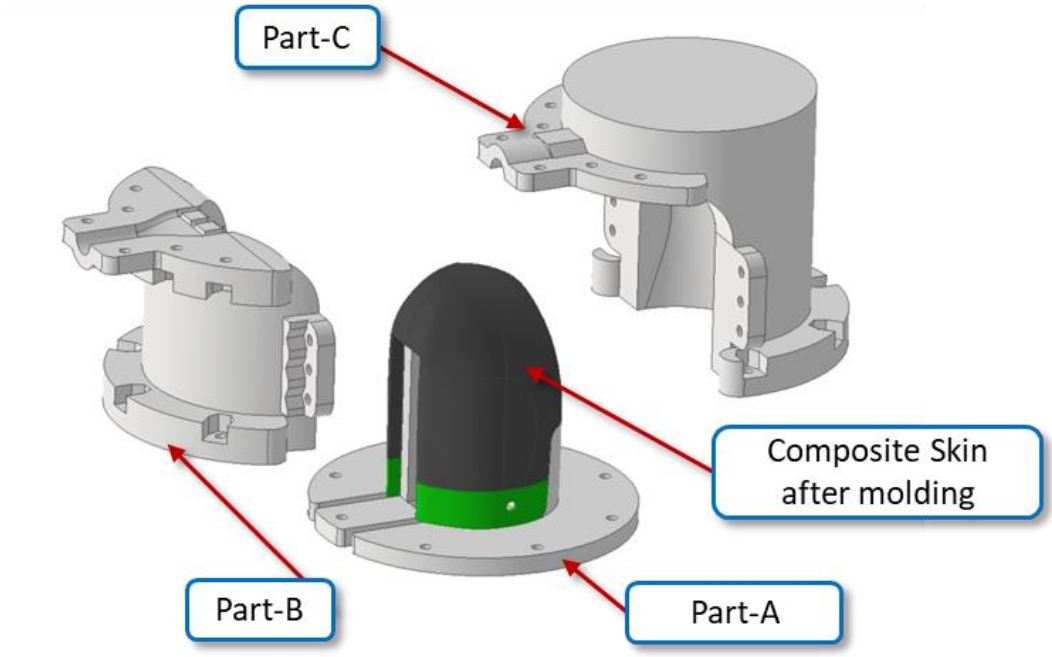

Fig 4.16 3-Part Mold for Composite Skin

Once molded the Ecoflex 50 is sticky and moist in nature. This may affect the behavior of the sensor by introducing hysteresis into the system. The object may stick to the surface of the FingerTac during object manipulation. This can lead the magnet to stick to the inner surface of the silicone layer and increase the delay in returning back to its original position.

To combat the hysteresis and improve the functional qualities of the outer skin layer, the silicone material was modified according to our requirements. The Ecoflex was mixed with SLIDE which is a liquid surface tension diffuser, that serves as an additive that profoundly influences the outcome of the curing process of silicone. Its primary function is to reduce the surface tension of the silicone once cured. This reduction in surface tension has several benefits, including the creation of a silicone surface with improved smoothness and reduced stickiness.

By incorporating SLIDE into the silicone mixture, the resulting cured silicone exhibited a notably lower surface tension. This property is advantageous for achieving a

smoother and more uniform outer skin layer. The use of SLIDE is a strategic choice to enhance the overall quality and appearance of the final silicone product.

In summary, the three blocks (Part A, Part B, and Part C) were intricately designed to shape the outer skin layer, while the addition of a black color pigment and SLIDE from Smooth-On played crucial roles in achieving the desired visual and tactile characteristics of the cured silicone. This meticulous approach to material selection and design contributes to the overall success of the outer skin layer fabrication. The FingerTac was manufactured and assembled.

4.4 Interchangeability of FingerTac:

FingerTac can be worn on a human fingertip as well as the fingertip of the Allegro hand as shown in the Fig.4.16. In the case of attaching the FingerTac on the Allegro Hand, a simple adapter was designed to fit inside the hollow shell of the FingerTac. FingerTac is fastened to the adapter with the help of M1.7 bolts.

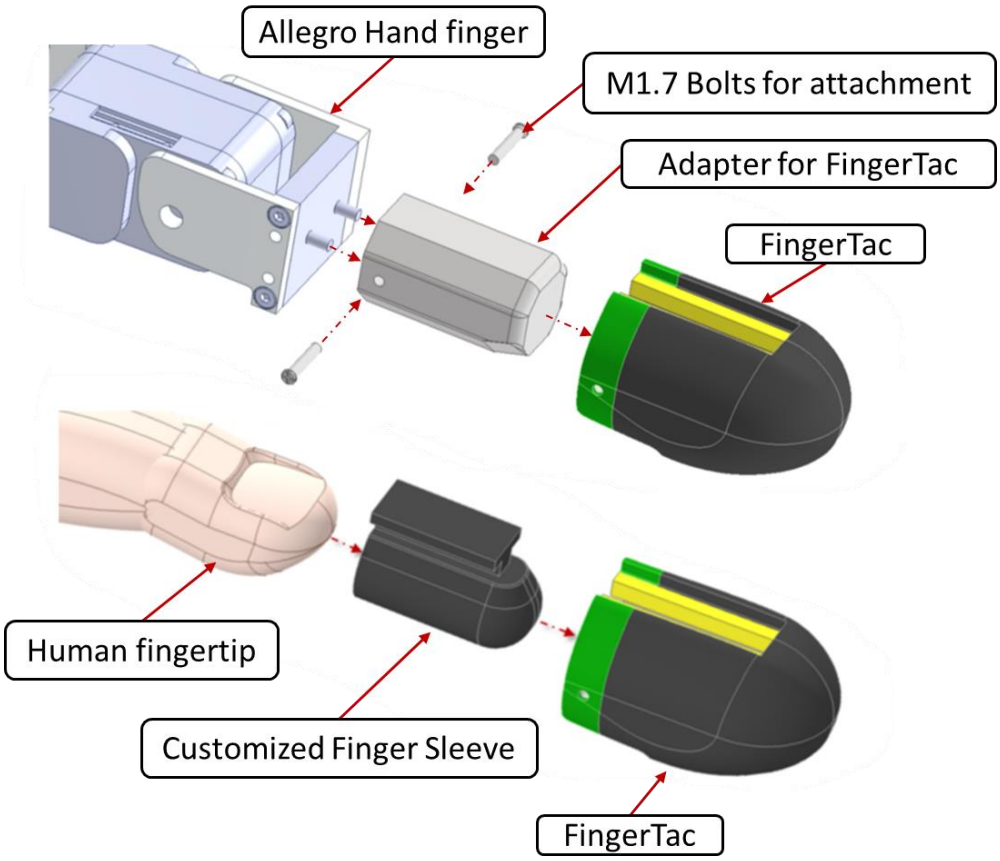

Fig 4.16 3-Part Mold for Composite Skin

4.5 Usage of FingerTac while manipulating an object:

FingerTac can be worn on the fingertip of the user to measure tactile data around the surface of the fingertip, as shown in the Fig.4.17.

In this scenario, the user wears the FingerTac device on their fingertip, and the device is equipped to sense and analyze tactile sensations during interactions with different surfaces. The two-fingered manipulation involves the user using two fingers, and the involvement of a ping-pong ball suggests a tactile interaction with a round and smooth object.

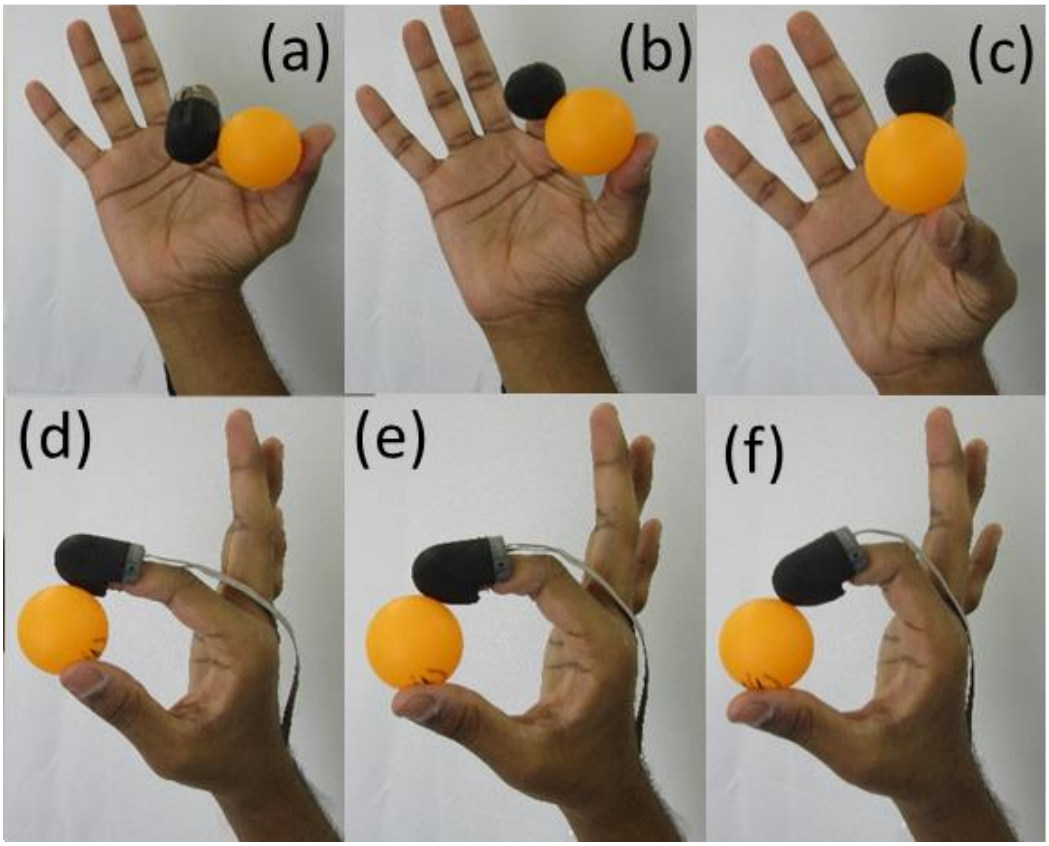

Fig 4.17 3-Part Mold for Composite Skin

4.6 Calibration of FingerTac:

Previous designs of the wearable tactile sensor as illustrated in the literature [2.9], [2.10], and [2.11] works on the finger pad deformation principle. The performance of deformation of finger pad depends upon the physical and biological characteristics such as softness and hardness of the finger pad of the fingertips. The sensor performance is dependent upon the displacement of magnet as it is directly dependent upon the characteristics of the finger pad. However, the current wearable tactile sensor design does not depend upon these factors as the user's fingertip does not come directly in contact with the object.

As there are no human biological parameters as mentioned earlier involved while measuring the force applied on the fingertips, the calibration for the current wearable tactile sensor need not be carried out each time the user wears the sensor on the fingertips. Computational modeling of silicone dome structure can be possible however it is challenging to perform, hence supervised learning was used to calibrate the sensor to 3-axis force values by converting the Hall-effect sensor raw data generated due to the application of the external force.

As a ground truth, a reference sensor was used to train and test the tactile sensor. The calibration was conducted in two phases. The first phase was the training phase where the tactile data was generated for curve fitting. A calibration matrix was created for the prediction of force values. The second phase was the testing phase which involved the generation of test data that acted as an input to the calibration matrix to estimate the force values.

The fingertip tactile sensor is evaluated by comparing the estimated force values to the true force values measured by the reference sensor. We used linear regression with a quadratic model quadratic linear regression model to convert the raw readings from the Hall-effect sensor to 3-axis force measurements. We worked with linear models during preliminary training. However, the estimated force values on the test data were not at par with the true force values measured by the reference sensor.

The evaluation of the FingerTac tactile sensor is conducted by comparing the estimated force values to the tue values of the force measured by the reference sensor. We used linear regression with a quadratic model quadratic linear regression model to convert the raw readings from the Hall-effect sensor to 3-axis force measurements. We worked with linear models during preliminary training. However, the estimated force values on the test data were not at par with the true force values measured by the reference sensor.

4.6.1 Calibration Setup of FingerTac:

The experimental setup for testing and calibration is shown in Fig.4.16. A 6-axis force torque sensor, ATI-Nano-17 from BL Autotech was used as a reference sensor to measure the actual normal and shear forces directly imparted by the user's fingertips. For this thesis only 3-axis forces were used for calibration of the FingerTac. A flat 3D printed surface was attached to the top of the BL-Autotech Force Torque sensor as shown in figure 4.18. The 3D-printed flat surface provides enough area for the user to comfortably apply normal and shear forces while wearing the fingertip tactile sensor. A base plate was also 3D printed to keep the reference sensor stable during the calibration process as shown in Figure 4.18. The base plate was mechanically fastened on a rigid table such that there is no relative motion between the table and the force-torque sensor. Fig.4.16 shows the overview of the calibration system in the form of a simple block diagram.

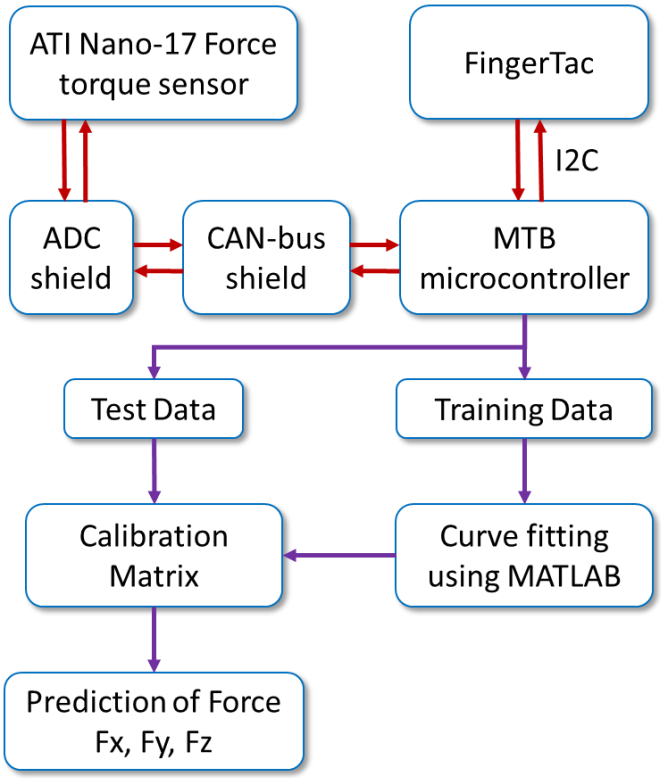

Fig 4.16 FingerTac Calibration setup

A raw data is sent to the microcontroller from the hall effect sensors which are embessed within a flexible PCB via the I2C communication protocol. The microcontroller used to receive the raw data is the MTB4 from IIT (Italian Institute of Technology). The analog data of the reference sensor is converted to digital data by using an Analog to digital converter and is sent to the microcontroller via the CAN bus communication interface. MLX90393 can be synced with the ATI Nano-17 using the CAN communication interfaced. Further, the digital data for each individual axes from the fingertip tactile sensor and the reference force-torque sensor's force measurements are sent from the microcontroller to the PC via a CAN-bus to Serial interface as shown in the Fig. 4.16. The readings from the MLX90393 and the ATI Nano-17 are collected at a sampling rate of 100Hz. To initiate the calibration process the readings are plotted against time for performing calibration.

4.6.2 Calibration Methodology of FingerTac:

The calibration methodology used to calibrate a single taxel will be illustrated in the upcoming section. As an example, taxel 11 is chosen for the calibration as it is often in contact with the flat surface mount during calibration. The location of the taxel can be seen in the Fig.4.17. It was observed that by applying force randomly to calibrate the sensor, the sensor gave out results that cannot be used for the prediction of force measurement. Therefore, a simple yet systematic procedure was followed to calibrate the fingertip tactile sensor.

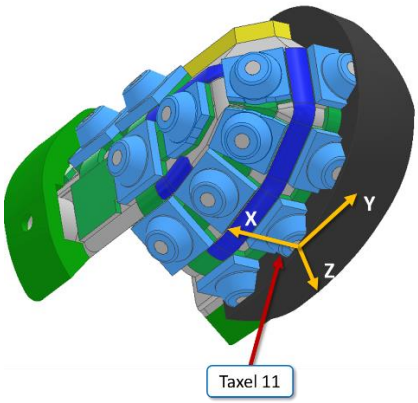

Fig 4.17 FingerTac Taxel 11

At first, a test subject chosen for using the sensor for acquiring training data was asked to sit in a relaxed position with their elbows supported on the table. Then the subject was asked to wear the custom finger sleeve to prevent the sensor from slipping off the fingertip before putting on the fingertip tactile sensor. The subject was then asked to try out the sensor by applying normal force in the Z direction by pressing down on the flat surface mounted on top of the reference sensor and applying shear force by making slight movements in +/-X and +/-Y directions while maintaining the normal force down on the flat surface as shown in the Fig 4.18.

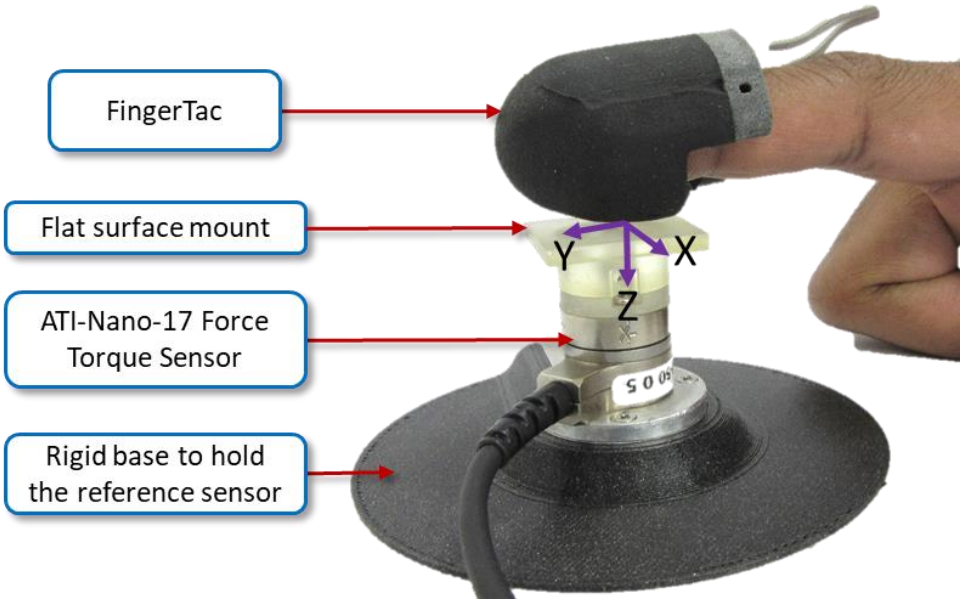

Fig 4.18 FingerTac Calibration Setup

A simple GUI was designed and provided as feedback to the user to view the resultant force values measured by the force-torque sensor. After conducting several functional trials by trying out the sensor a couple of times the user was asked to initiate the calibration process by applying normal and shear forces in an oscillatory fashion i.e. sequentially increasing and decreasing the magnitude of Z, -X, +X, -Y, and +Y forces. Fig.4.19 shows the training data recorded by the subject while conducting training data acquisition. Solid lines show the data measured by the force torque sensor while the dotted lines represent the force estimated by the FingerTac. For now we ask the reader to focus on the solid lines, which show the data from the force-torque sensor.

Similar to the training, in the data acquisition procedure the subject was asked to sit in a comfortable and relaxed position with the elbows supported on the table. The subject was then asked to apply sequentially increasing and decreasing magnitude of shear and normal forces in all axes. It was observed that it was difficult to apply forces of more than +/-2 N of shear force. Hence for the shear force, the subject was asked to apply forces between 0 and +/-2 N. While capturing the test data an additional instruction

given to the subject was to maintain the magnitude of force which the subject can apply with ease between the above-mentioned magnitude limits for a period of around 5 seconds before changing the force magnitude. Fig. 4.20 shows the testing data captured by the subject while performing the test data acquisition procedure.

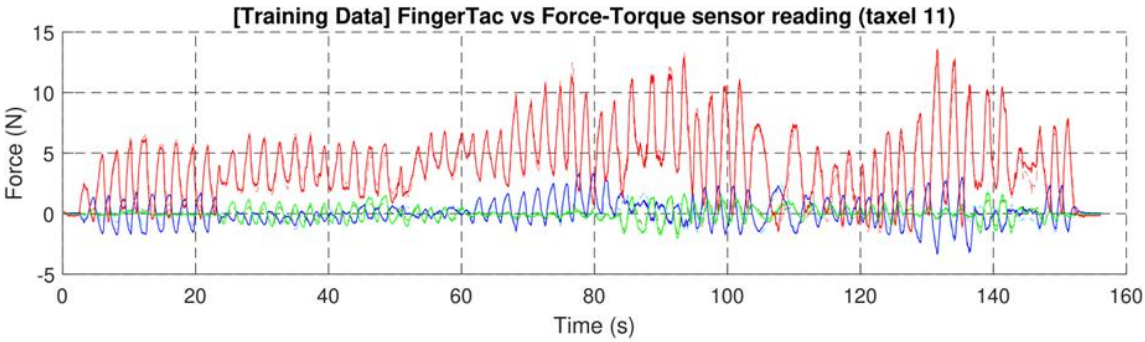

Fig 4.19 Calibration data for Training

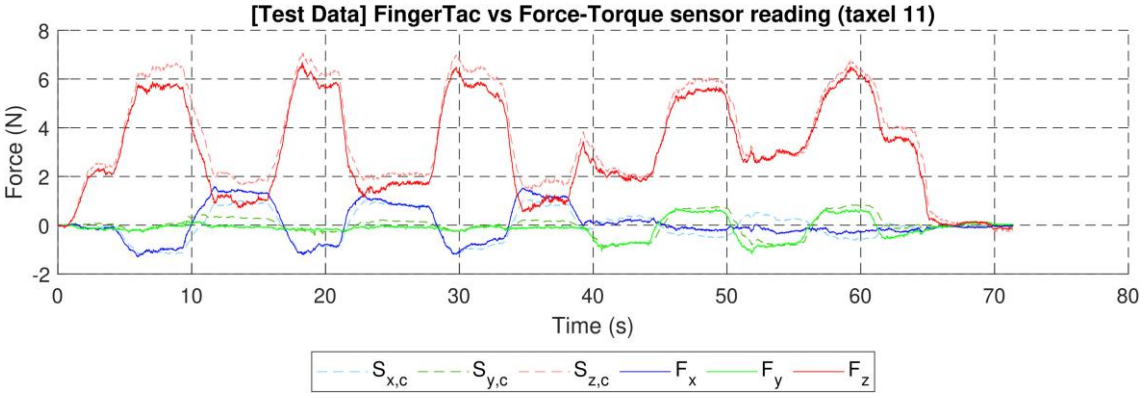

Fig 4.20 Calibration data for Testing

4.6.3 Calibration Results of FingerTac:

The results of the calibration for the training data can be seen in Fig.4.19 and test data can be seen in Fig.4.20. In both figures, the solid blue, green, and red lines represent the 3-axis force data measured by the force-torque sensor in X, Y, and Z directions, respectively. The dotted blue, green and red lines represent the predicted outputs of the

regression model in the X, Y, and Z directions, respectively. Looking at the result of calibration performed for training data in Fig. 13, we can see that the predictions from the polynomial regressions (dotted lines) are coincident with the actual force values (solid lines) for most time steps. In Fig.4.20 we can see the result for the test data. Here we can observe that the dotted lines tend to follow the actual force values measured by the force-torque sensor with some slight deviation. In the case of the Z-axis measurements, we can observe a slight overestimation. In X and Y axis the deviation from the actual measurements were lower compared to the Z-axis. The mean absolute error and root mean squared error per axis were calculated and are presented in Table I below. We can observe that both, mean absolute error and root mean squared errors for all the axes are very low. The errors observed in the Z-axis is slightly higher than the error observed in the X and Y axis. This might be due to higher forces measured in the Z-axis. Overall, the low error values indicate that the tactile sensor can measure contact forces while handling objects.

TABLE I Mean Absolute Error Calculated Per Axis

Axis	**X**	**Y**	**Z**
MAE	0.21N	0.16N	0.44N

4.7 Conclusion and Discussion of FingerTac:

In this chapter we presented the design of a wearable fingertip tactile sensor named FingerTac. The design allows the user to measure tactile information not only while grasping an object but also while performing object manipulation.

A sensor taxel was calibrated to true force values and compared with an industrial-grade force-torque sensor. The calibration yielded good results proving that the sensor can be calibrated to measure 3-axis force applied by the human fingertips. However, we believe that for skill transfer the calibration of all taxels is not required, as FingerTac can be also applied to robot hands, i.e. the Allegro hand, and reproducing the uncalibrated sensor measurements might be sufficient. A lot of recent research in tactile sensing for robots uses uncalibrated sensor measurements [6.1].

In future work we plan to apply FingerTac to several human fingers and use it for skill transfer from humans to robots. Other possible future applications include skill transfer from human experts to non-experts and monitoring of humans, for example for quality control and optimization of products such as screw caps.

Chapter 5

ExoGlove Version 2 -

5.1 Introduction:

ExoGlove Version 2 is a mechanical glove which is worn on top of the user's hands to trac the motion of the fingers. The ExoGlove Version 2 is integrated with the FingerTac thereby it is able to track the position and orientation of the wearable tactile sensor while manipulating the object. The ExoGlove Version 2 has a different mechanical design as compared with the ExoGlove Version 1. One of the objectives of the ExoGlove Version 1 was to support the wearable tactile sensor modules which have been distributed over the finger segments. Hence it utilized a Remote Center of motion mechanism to achieve a rotation about the finger joints. This increased the stability of the wearable tactile sensors however; it also increased the overall bulkiness of the device. The device had a complicated four bar linkage which was susceptible to loosening and hence required constant maintenance. Overall the mechanism was heavy for the user to utilize rendering it impractical for applications such as in-hand manipulation.

On the other hand the ExoGlove Version 2 consisted of an articulated linkage mechanism which was designed as compact and lightweight structure. The mechanism consisted of a planar four bar redundant linkage which was designed using the CAD tools. The mechanism was designed such that it followed the movement of the fingertip during flexion and extension. Unlike the ExoGlove Version 1 the ExoGlove Version 2 was able to achieve complete flexion and extension of the finger while manipulating the object. The ExoGlove Version 1 featured a compact Hall -Effect based encoder which

was embedded in a PCB with the small possible form factor. The Encoder was integrated with its mechanical casing allowing it to be embedded into the rotary joint of the two corresponding linkages of the ExoGlove. The next section describes the Mechanical and Electronic design of the Hall-Effect based encoder.

5.2 Electronic design of Hall-Effect based encoder:

This section provides the encoder design in detail. It provides the design steps used for the electronics and the thought process behind making the Hall-Effect based encoder making it a practical solution for measure the angular data.

5.2.1 Working Principle:

A diametrically magnetized permanent magnet is suspended concentric to the center of the axis of the Hall-Effect sensor as shown in the Fig.5.1 below. The magnet is made to rotate in clockwise or anticlockwise direction. The Hall effect sensor measures the raw values of the encoder which can be calibrated to angular measurements using mathematical modeling.

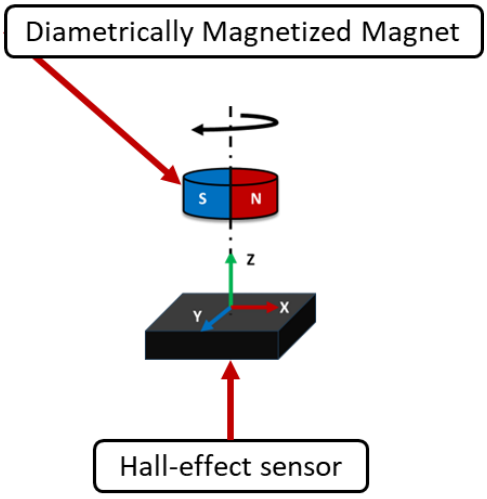

Fig 5.1. Hall-Effect based Encoder Working Principle

This encoder can work as an absolute encoder as it can identify the direction of rotation as well as count the number of rotations performed. In our case similar arrangement was used to measure the absolute position of the magnet while being rotated.

5.2.1 Encoder PCB design:

As the FingerTac is also a Hall-effect based wearable tactile sensor which utilizes the Hall-Effect sensor IC MLX90393. Therefore for the Encoder, the MLX90393 was chosen as the Hall-Effect sensor to measure the position of the rotating magnet. This simplified the overall system designed instantly as the same schematics used for routing the FingerTac's Hall-Effect based flexible PCB was used in case of the encoder PCB design. However, to reduce the mechanical size of the sensor the PCB was designed with the form factor as small as possible. A Daisy chain arrangement was utilized for the Pinouts of the Encoder PCB. This increased the ease of routing within the ExoGlove and also reduce the complexity associated with the PCB design. The wire routing within the PCB was routed in the I2C protocol configuration as shown in the Fig 5.2. below.

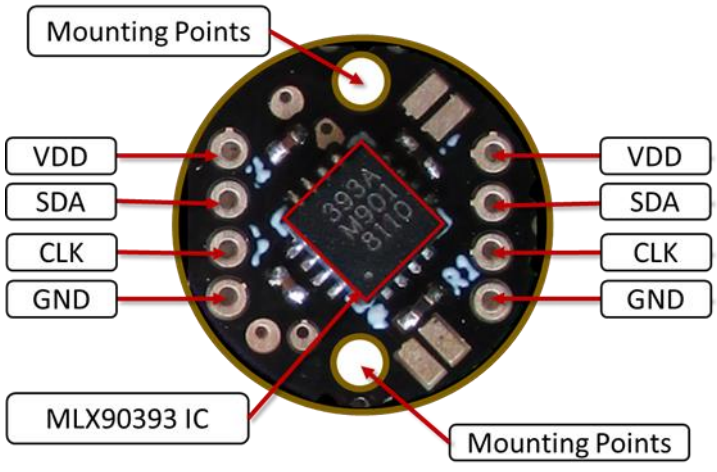

Fig 5.2. Hall-Effect based Encoder PCB.

Overall, the encoder PCB was manufactured with thin profiles roughly 1.5 mm in

diameter. The Diameter of the PCB was 11 mm. To mount the PCB in the encoder casing two mounting holes were provided. These acted as a guide for the PCB to stay fixed in position. The MLX90393 Hall-Effect sensor PCBs are comprised of four addresses in total namely, 00, 01, 10, 11. Hence the Encoder routing for every PCB was different as these addresses were selected while creating the schematic of the Encoder PCB. Hence the PCBs were manufactured in pairs of four. Each pair having a different batch of manufacturing order.

5.3 Mechanical design of Hall-Effect based encoder:

To have a compact form factor the hall effect sensor a minimalist design criterion was followed. The mechanical design of the encoder was designed to achieve a compact form factor.

5.3.1 Design Principle:

To achieve a compact form, factor a simple design principle was followed. The mechanical design of the PCB should have minimum rotating or moving parts. It should be as thin as possible. Overall, the encoder casing should be such that it would act as a simple revolute joint between the two consecutive mechanical linkages of the encoder. also it was necessary to make sure that the encoder joint acted as a revolute joint which would not wobble during rotation. Wobbling would create ripples in the magnetic field in random directions inducing errors inside the encoder system.

5.3.2 Encoder casing and shaft design:

Encoder casing and shaft design were the key mechanical components of the mechanical design of the encoder. The casing was designed and iterated many times. However, finally a design generated was thin and minimalist in nature. Initially it was decided to place the suspending the magnet at the height of 1.5 mm from the surface of the Hall- effect sensor PCB. The diametrically magnetized permanent magnet was chosen as 1.5 mm in diameter. To embed the permanent magnet an encoder shaft was designed. The shaft was made hollow to for the diameter of the magnet. A pressure fit tolerance was created between the magnet and the hollow shaft. This ensured that the magnet and the encoder shaft to be snuggly fit inside the hollow shaft without being loosened. To prevent the bearing from wobbling a SMF85 cageless bearing from

Kitanihon Seiki was chosen as a perfect match. The outer diameter of the bearing was 8 mm with the inner diameter being 5 millimeters. The cageless design of the bearing allowed for minimum thickness. The thickness was around 2 millimeters.

Multiple designs of the casing were realized. These designs were iterated multiple times changing the designing features. Overall, it was decided that the top surface of the Hall-Effect sensor PCB was to be used as a base to align the casing on the Hall-Effect sensor PCB the bottom part of the casing was cut was a square shaped groove with the edges having a slide fit tolerance. This prevented the PCB from moving laterally and being displaced in the normal direction. Further the bottom side of the casing was equipped with two cylindrical extrusions which were designed to have the same diameter as the mounting holes on the Hall-Effect based PCB. The cageless bearing mentioned in the earlier paragraph was sandwiched between the Casing and the hollow shaft. The Casing was designed such that the bearing would be flushed inside the top surface of the casing. This would allow for a more compact design of the encoder. Fig 5.3 showcases the exploded view of the Hall-effect based encoder assembly.

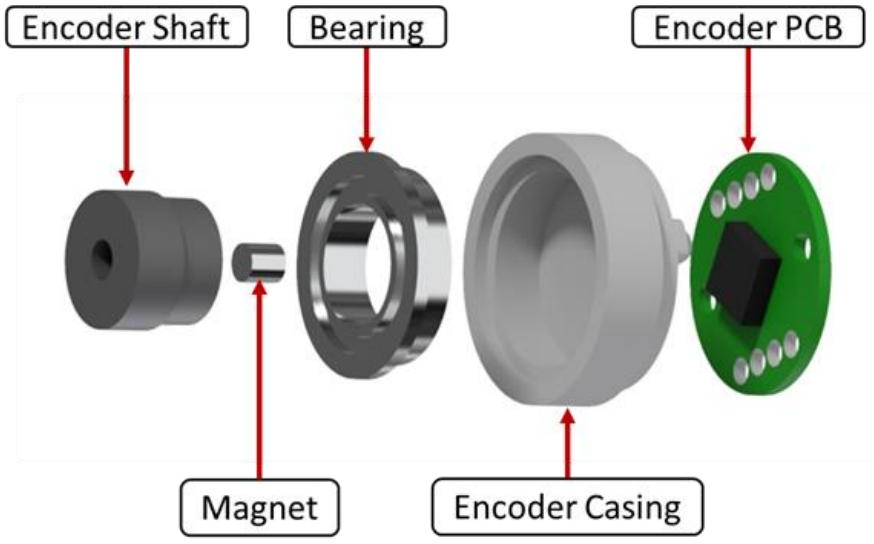

Fig 5.3. Hall-Effect based Encoder PCB.

5.4 Mechanical design of ExoGlove Linkages:

Overall the mechanical design of the linkages was designed keeping in mind that the ExoGlove should be light weight and compact. Also it was made sure that the Mechanical design should have around four degree of freedom with the sizes of the linkages being enough to accommodate complete flexion and extension of the finger.

5.4.1 Design Principle:

One of the objectives of the ExoGlove was to map the position of the FingerTac to the Allegro hand. The allegro hand by Wonik Robotics is larger than the human hand and consists of only four fingers with each actuated by a servo motor. To maintain the similarity between mechanical configurations of ExoGlove and the Allegro hand, a set of only four mechanical fingers was designed for the ExoGlove.

Each finger of the ExoGlove consisted of a set of four linkages arranged in an articulated linkage design as shown in Fig. 5.4. The dimensions of the linkages were designed such that complete flexion and extension of the user's finger was possible. It was necessary to also ensure that there is no hindrance while flexing and extending the finger while wearing the ExoGlove.

Autodesk Inventor was chosen as the CAD design software of the designing the mechanical linkages. The concept was designed initially using sketching tools of the Autodesk inventor. A sketch model of the fuser's finger was created in the sketch design along with arbitrary linkages lengths. The fingerTac was also modeled in the sketch to have higher dimensional accuracy. It was initially decided to have a link 4 designed as a universal joint. Even thought this seemed compact at first it was realized that the linkage designed were becoming longer. Hence the Universal Joint concept was

scrapped.

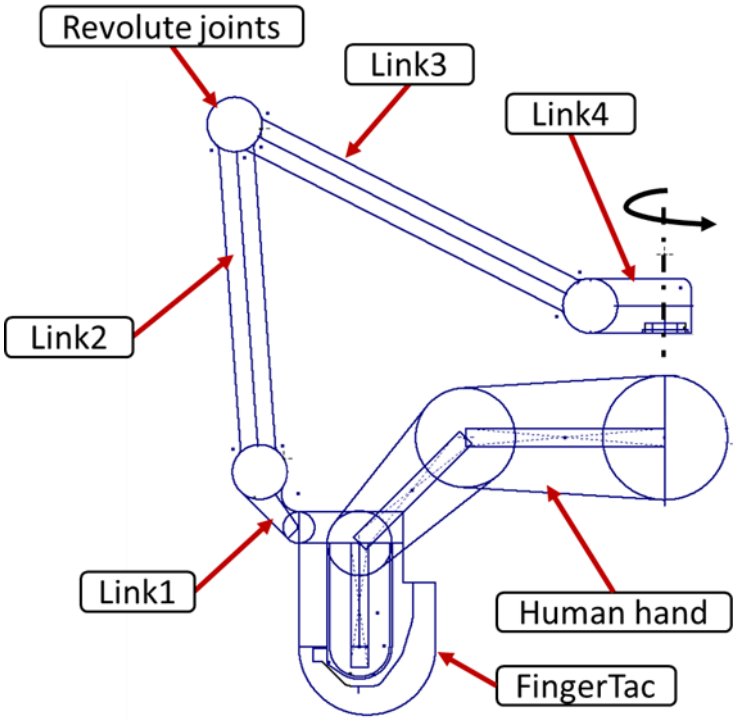

Fig 5.4. Hall-Effect based Encoder PCB.

5.4.2 Linkage Design:

Inspired from the design presented in these literature [5.1], [5.2]. The four bar linkage design ensured 4 degrees of freedom that enabled complete flexion, adduction, and abduction of the human fingers as shown in Fig. 5.5 and Fig. 5.6. To ensure that the weight of the linkage design is kept as low as possible, pockets were cut out from the linkages to lower the weight of the linkages. Overall a minimalist design approach was used to design the linkages between every revolute joint. To further reduce the weight every revolute joint comprised of only a single bearing. Overall the 4-linkage mechanism for every finger was designed such that the user would feel minimum hindrance or weight of the ExoGlove linkages while handling objects

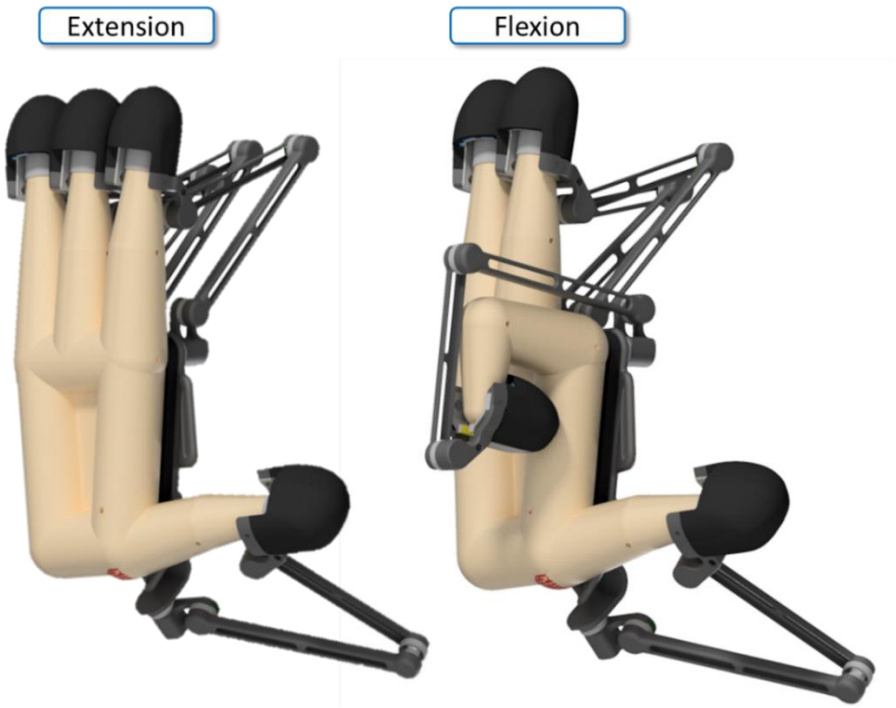

Fig 5.5. Flexion and Extension of ExoGlove

Fig 5.6. Adduction and Abduction of ExoGlove

5.5 Assembly:

Overall, a simple assembly process was used to assemble the components of the ExoGlove together. This section also highlights the integration of the ExoGlove with FingerTac.

5.5.1 Embedding revolute joint with encoders:

The mechanical linkages as shown in Fig. 5.4 are connected with each other using revolute joints. The encoder assembly shown in Fig 5.3 forms an integral part of the revolute joint mechanism. Each encoder was sandwiched between two mechanical linkages as shown in Fig. 5.7. Link3 houses the encoder casing and PCB and Link2 houses the Encoder shaft. Interference fit tolerance was used to snap-fit the encoder with linkages.

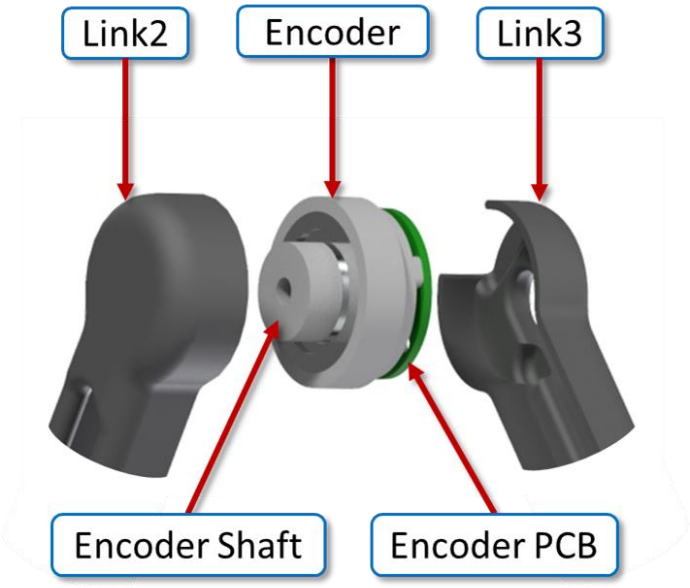

Fig 5.7. Adduction and Abduction of ExoGlove

5.5.2 Integrating FingerTac with ExoGlove:

Fig.5.8 illustrates the way FingerTac is assembled to the ExoGlove. Combining the ExoGlove to the FingerTac, we would be able to track its position and orientation while performing in-hand manipulation tasks.

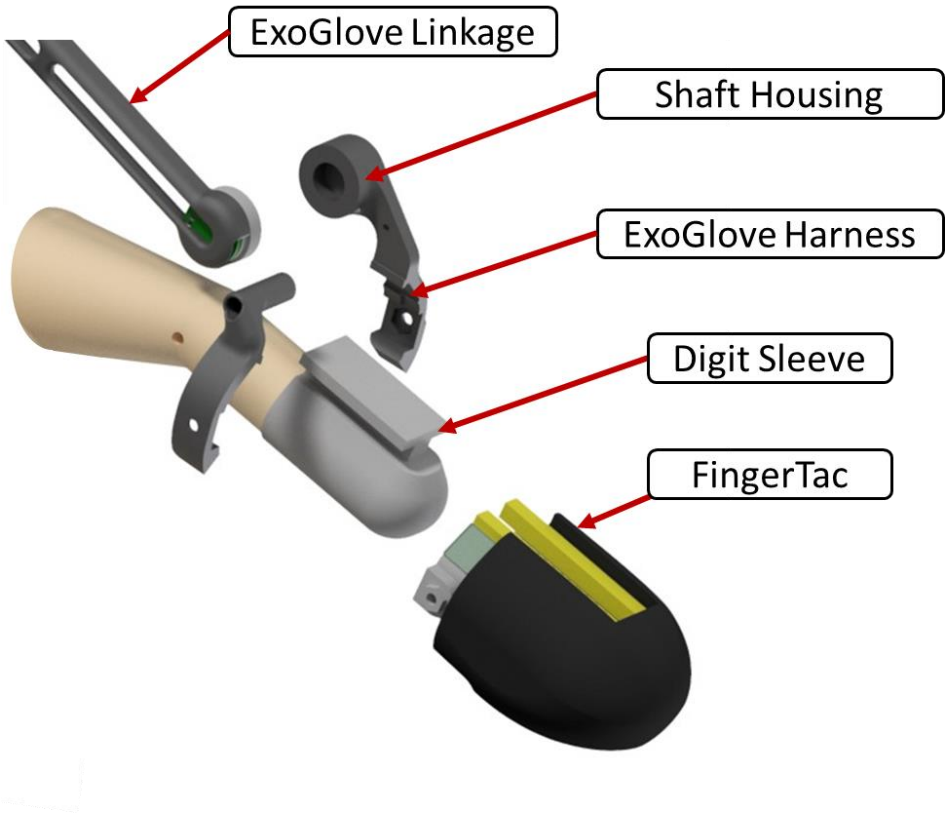

Fig 5.8. Integrating FingerTac with ExoGlove

5.6 System Design:

Fig. 5.9 illustrates the system design of the ExoGlove. Each finger of the ExoGlove was comprised of four encoder PCBs having independent addresses (Binary address: 00,01,10,11). The four encoders were connected on a single SDA(data line) as shown in Fig. 12. MTB-4 Microcontroller from IIT(Italian Institute of Technology) was used to communicate with the encoders. MTBs featured five I2C connections along with a CAN bus module to communicate with other devices such as PCs MTBs etc. By using the I2C communication, wires within the ExoGlove were reduced. The MTB used the CAN bus module to transfer the data measured by the encoders to the PC.

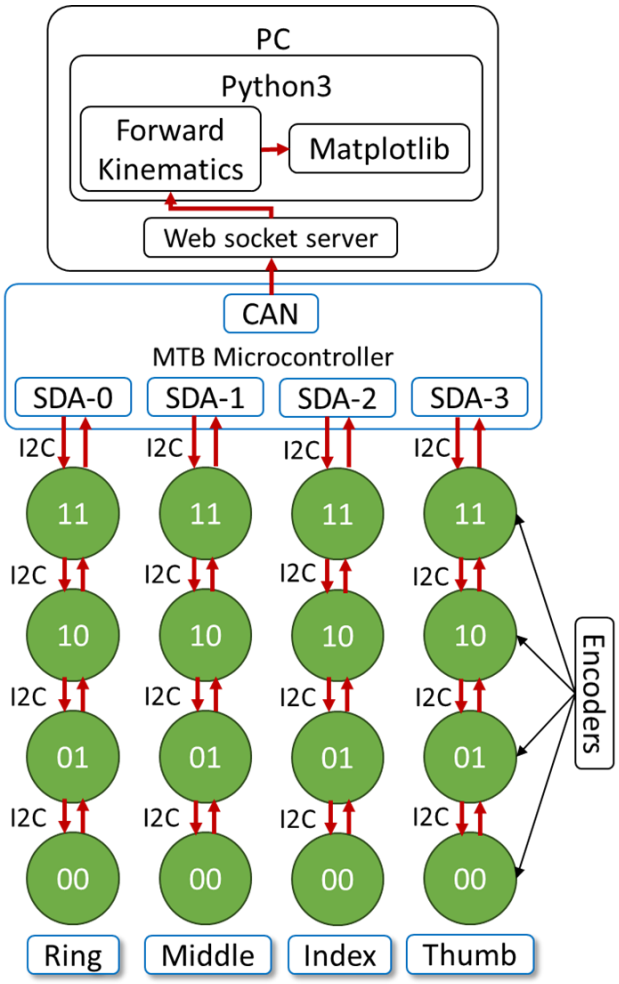

Fig 5.9. ExoGlove System Design

5.7 Software Description:

A WebSocket server was used to sort the incoming data by their respective addresses of the encoder. Two Python scripts were created to operate on the incoming raw data from the encoder. First Python script was written to calibrate and convert the incoming raw data to angle measurement for each encoder between -180 to 180 degrees. The second Python script contained a forward kinematic model of the linkage design of the ExoGlove along with a function used for real-time visualization of the forward kinematic model. The first Python script would transfer the calculated angles to the second Python script. The second Python script would use the incoming angle data to calculate the FingerTac position and at the same time provide real-time visualization of the forward kinematic model. The Matplotlib Python library was used for visualization.

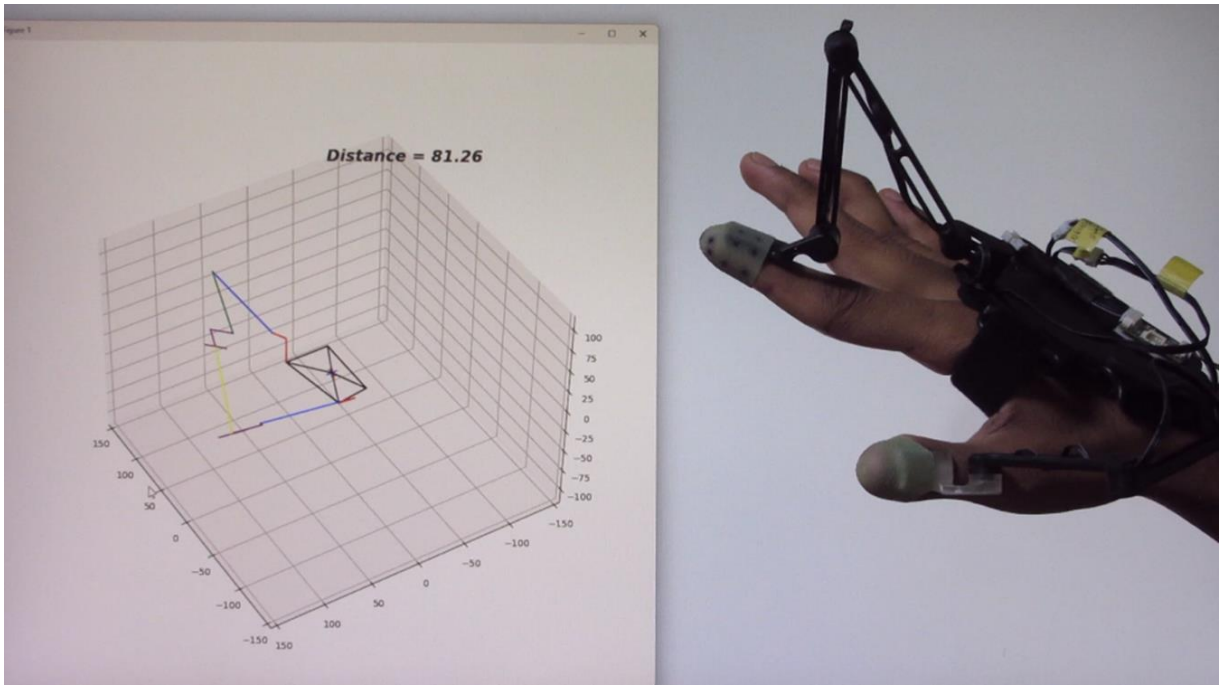

Fig 5.10. ExoGlove with Real time Visualization software.

5.8 Sensor Calibration:

The mechanical and electronic components of the encoder were assembled manually by hand. Therefore, the characteristics of the encoder varied depending upon the assembly of the encoder. In order to maintain the operational similarity between all the assembled encoders, it was necessary to calibrate the Hall effect sensor before calculating the joint angles. The objective of the calibration was to measure the operating range of the magnetometer. The X-axis and Y-axis raw magnetic data (Raw-X and Raw-Y) was measured by spinning the encoder shaft by one rotation. Algorithm 1 shown in figure 5.11 was used to calculate the peak values in X and Y axes (Peak-X and Peak-Y) and the Y axis normal value (Y-Normal)

Algorithm 1 Calibration Procedure for Joint encoder

Input Raw-X and Raw-Y.
Output Peak-X, Peak-Y, and Y-Normal

1: Record and store Raw-X and Raw-Y values for 1 rotation.
2: Find Max-X and Min-X values from recorded Raw-X.
3: Calculate Mid-X = (Max-X + Min-X)/2.
4: Find Max-Y value and Min-Y values from recorded Raw-Y.
5: Calculate Mid-Y = (Max-Y + Min-Y)/2.
6: Calculate Peak-X = Max-X - Mid-X.
7: Calculate Peak-Y = Max-Y - Mid-Y.
8: Calculate Y-Normal = Peak-X/Peak-Y.

Fig 5.11. Calibration Procedure for Joint encoder.

Algorithm 2 as shown in the Fig. 5.12 is proposed to calculate the Angle of the encoder shaft. The angle is obtained by using the following equation:

$$\theta = arctan2\left(\frac{Real-Y}{Real-X}\right) \qquad (1)$$

Here the Real-X and Real-Y values are the X and Y intercepts calculated as per Algorithm 2

Algorithm 2 Calculating Joint Angles in range of 0 to 360 Degrees

Input Raw-X, Raw-Y, Peak-X, Peak-Y, and Normal-Y.
Output Angle.

1: Calculate Real-X = Raw-X - Mid-X value
2: Calculate Real-Y = (Raw-Y - Mid-Y) x Normal-Y
3: Calculate Angle = atan2(Real-Y/Real-X)
4: **if** $Angle \leq 0$ **then**
5: Angle = Angle + 360
6: **end if**

Fig 5.12. Calculation of joint Angles in range 0 to 360 degrees.

5.8.1 Experimental setup:

To test the behavior of the encoder a simple experimental setup was designed. The experimental setup consisted of an encoder placed in the center of the setup shown in Fig. 5.13. 10 degrees angle markers were marked around the encoder casing. To store the measured raw magnetic data from the magnetometer, the joint encoder was connected to the PC via a microcontroller. The encoder shaft was fitted with a 3Dprinted pointer. The experiment was conducted in two steps. The first step was to calculate the calibration parameters (Peak-X, Peak-Y, and Normal-Y values) by performing the calibration. To perform the calibration, the encoder shaft was spun for one rotation, and Algorithm 1 was used to calculate the calibration parameters. The next

step was to evaluate the sensor by comparing the measured encoder angle (Angle) with the corresponding angle markings. The angle was measured at every 10 degrees. For every 5 seconds, the encoder shaft was rotated by aligning the tip of the pointer with the angle marker.

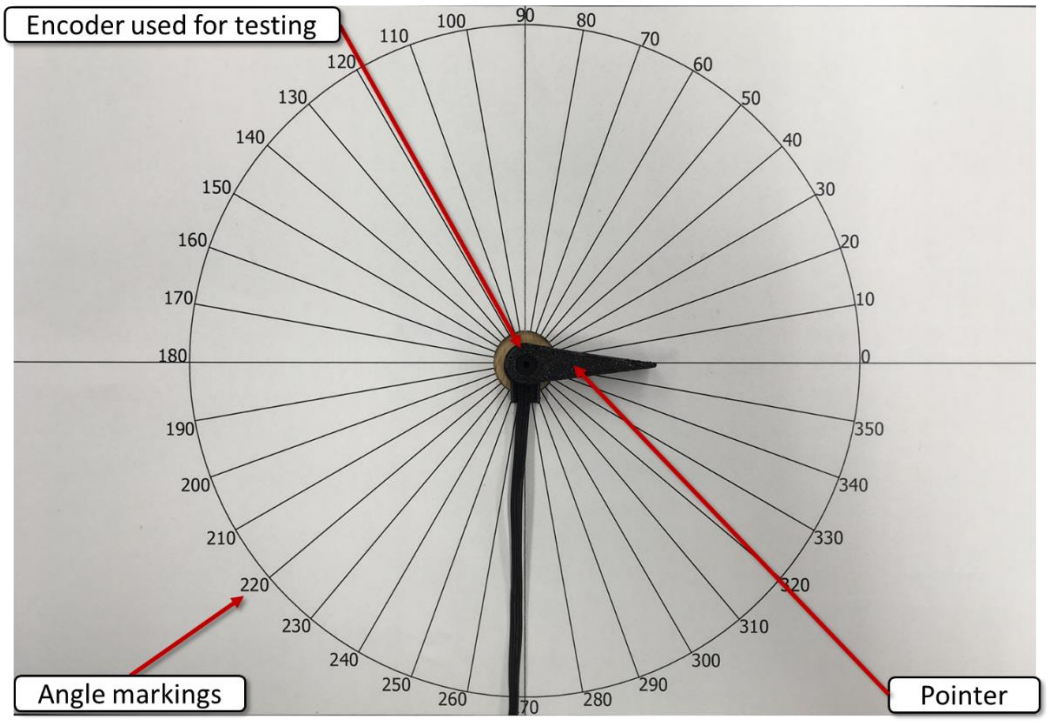

Fig 5.13. Calibration setup of the Encoder.

5.8.2 Calibration results:

The results of the evaluation process can be seen in Fig. 5.14. As expected the angle measured by the proposed joint encoder shown in red overlaps the true angle plot shown in blue for almost all angles. However, there is a slight deviation observed in the middle, roughly between 120 and 240 degrees. Overall the plot shows a linear relationship between the encoder angles measured at specific time intervals similar to the true angle plot. The mean absolute error was calculated by using equation 2.

$$MAE = \sum_1^n \left(\frac{|y_i - x_i|}{n}\right) \qquad (2)$$

Here the y_i represents the predicted angle value in this case the angle measured by the proposed joint encoder. xi represents the true angle value. The mean absolute error was calculated as 2.76 deg.

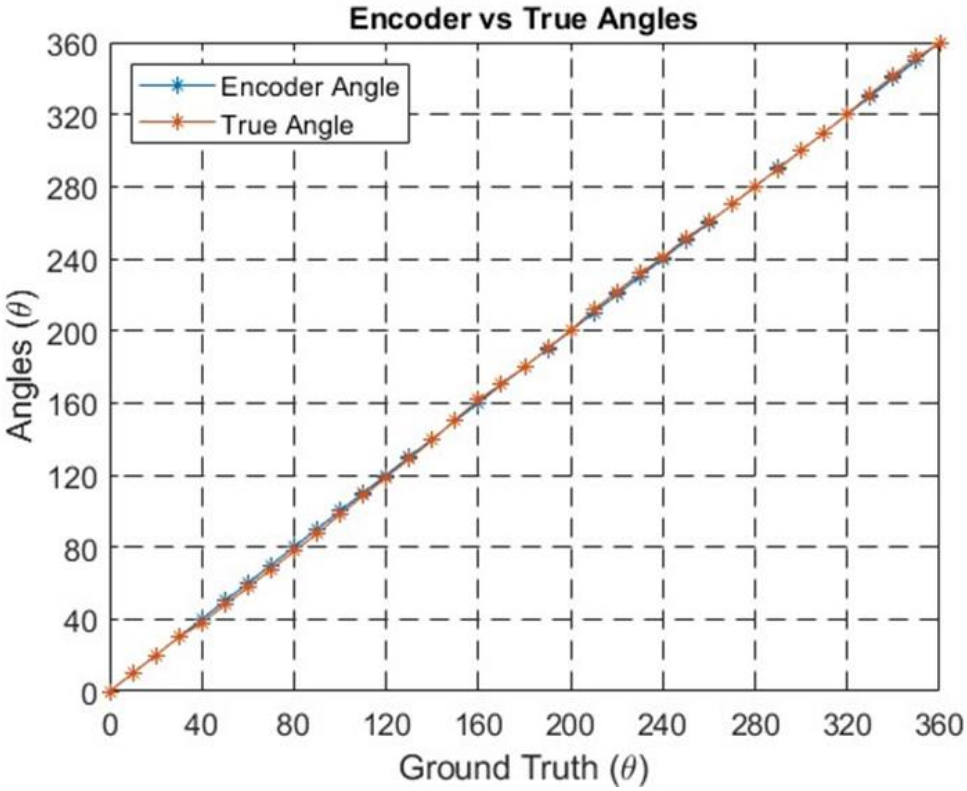

Fig 5.14. Calibration result of the Encoder.

5.9 Evaluation of ExoGlove forward Kinematic model:

5.9.1 Experimental setup:

As mentioned earlier the main goal of the ExoGlove was to map the position of FingerTac to the Allegro hand. However, first, we must evaluate the forward kinematics model of the ExoGlove. In this paper, we evaluate the ExoGlove kinematic model by measuring the distance between the fingertip and the thumb by performing forward kinematics. Objects of different shapes (cuboidal, spherical and cylindrical) were chosen as samples for the experiment as shown in Fig. 5.15, 5.16 and 5.17. We used the ExoGlove as a measurement device by holding each sample between the thumb and index fingertips and compared the measured length between the fingertips (thumb and index) with the actual dimension (height, width or length) of the object as shown in the Fig.5.15.

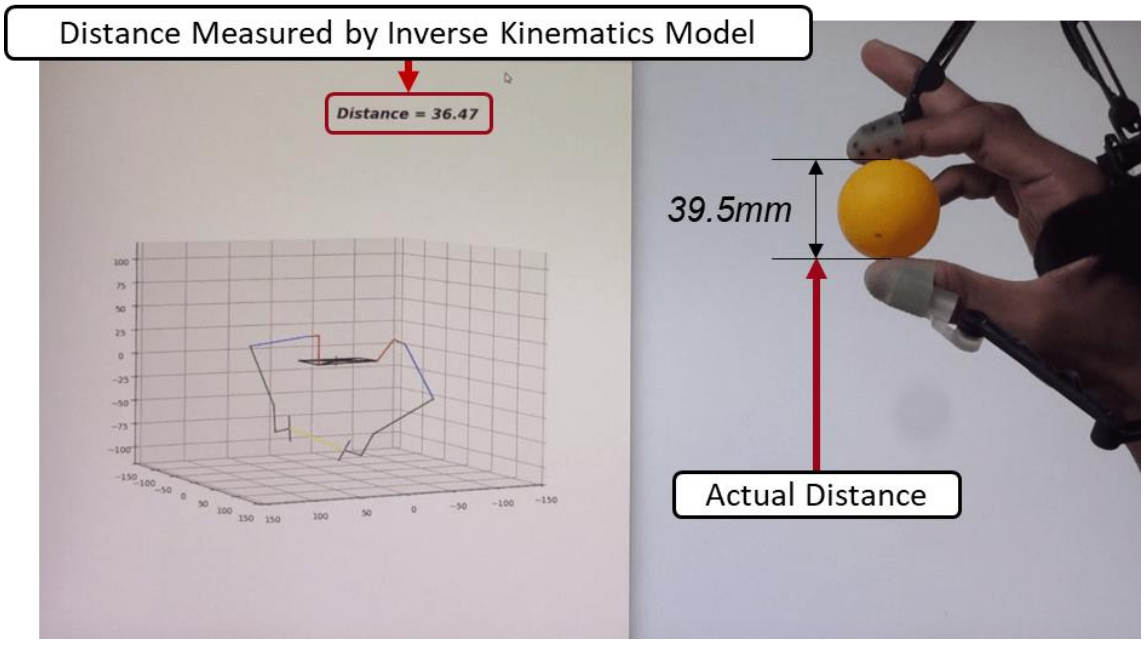

Fig 5.15. Calibration result of the Encoder.

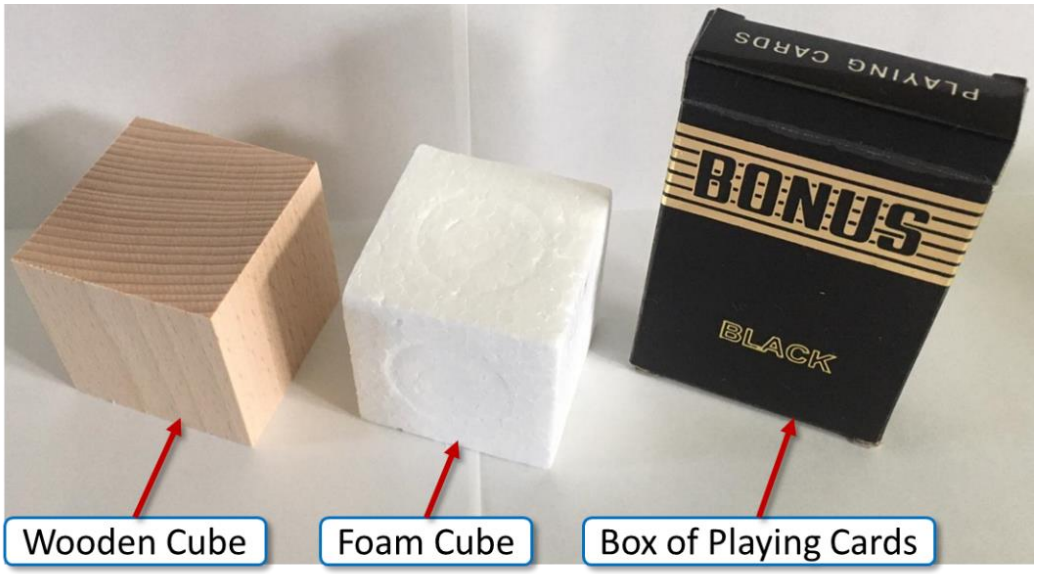

Fig 5.16. Cuboidal shaped objects used for the experiment.

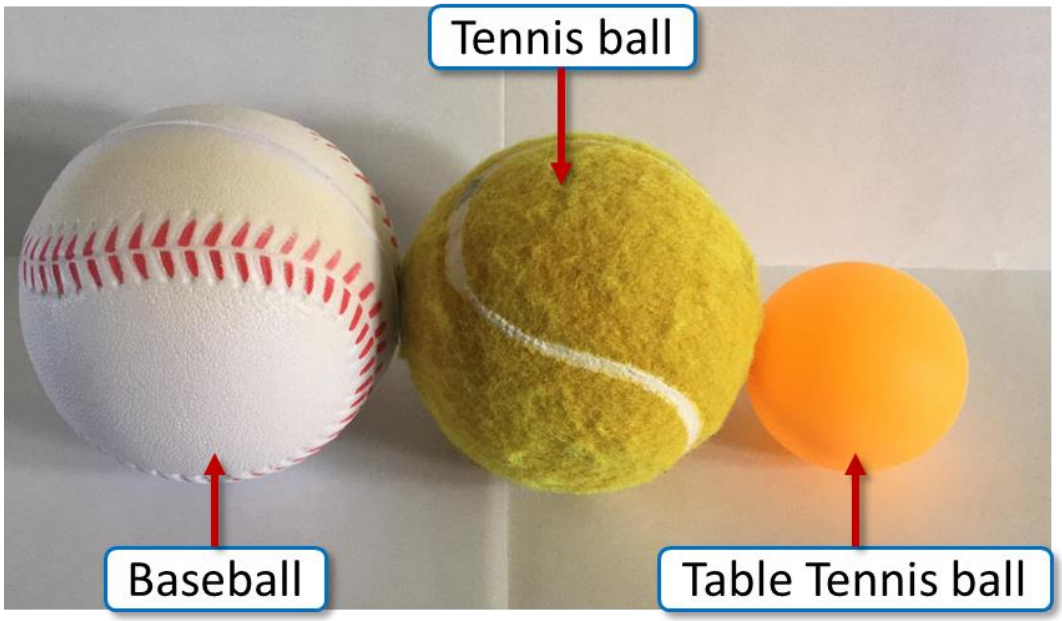

Fig 5.17. Spherical shaped objects used for the experiment.

Fig 5.18. Cylindrical shaped objects used for the experiment.

5.9.2 Evaluation Results:

By observing the measured dimensions and comparing them with the actual dimensions as shown in the Table I, II and III we can say that the ExoGlove can accurately measure the different dimensions of a sample further indicating that the Forward kinematic model can be used to map the FingerTac position to the Allegro hand. The mean absolute error between the actual and measured dimensions was calculated as approximately 3.8 mm.

Table I: Measuring of cuboidal shaped objects

Cuboidal Shaped Sample	**Actual**	**Measured**
iPhone SE Width	58.5 mm	~ 54 mm
Box of playing Cards Height	61 mm	~ 60 mm
Wooden Cube Height	50 mm	~ 46 mm
Foam Cube height	48.8 mm	~ 45 mm

Table II: Measuring of cylindrical shaped objects

Cylindrical Shaped Sample	**Actual**	**Measured**
Wooden Cylinder Height	50 mm	~ 47 mm
Wooden Cylinder Diameter	49 mm	~ 43 mm
Coffee Mug Diameter	80 mm	~ 77 mm
Calligraphy Brush Diameter	12.5 mm	~ 10 mm

Table III: Measuring of spherical shaped objects

Spherical Shaped Sample	**Actual**	**Measured**
Table Tennis Ball Diameter	39.5 mm	~ 36 mm
Tennis Ball Diameter	64 mm	~ 58 mm
Base Ball Diameter	69 mm	~ 64 mm

5.10 Discussion:

The calculated mean absolute error for the proposed encoder joint is smaller than the mean absolute error of the Cyberglove [5.3]. The Cyberglove is widely used by researchers for measuring the joint angles of the human hand. The lower error observed for the joint encoders indicates that the joint encoder can be used effectively to measure the joint angles of the human hand. Sim et al. [5.4] suggest an error threshold of less than 5 degrees for the effective use of a data glove in a VR application. The error observed for the joint encoder is within this threshold indicating that the ExoGlove can be used effectively for VR applications also. The error of 3.8 mm observed in the forward kinematic model experiment can be explained due to the slight error observed in the encoder. Furthermore, the distance between the fingertips also depends on the point of contact of the fingertip while holding the object. Bending or torsion within the 3D printed structure of the ExoGlove may also give rise to error in calculation of the distance measured between fingertips. This can be improved with better structural design and the use of sturdier materials.

5.11 Conclusion:

This chapter introduces the ExoGlove, detailing its design and development. It also provides an assessment of the encoder in conjunction with the forward kinematic model. The incorporated mechanism facilitates seamless adduction and abduction finger movements for the user. The suggested encoder proves its effectiveness in accurately measuring joint angles. In future endeavors, we aim to demonstrate how the ExoGlove can be utilized to map human hand actions onto the Allegro hand. Additionally, we intend to explore the potential for skill transfer in forthcoming research.

Chapter 6

Discussion

6.1 Introduction:

This thesis illustrates the design and development of the wearable ExoGlove Version 1, followed by the design and development of the wearable fingertip tactile sensor, FingerTac, and finally the design and development of wearable ExoGlove Version 2.

6.2 Necessity of developing ExoGlove Version 1:

The wearable tactile sensor developed previously was a clamp-like design allowing the sensor to be clamped on of the finger segments. This method exposed the finger pad area of the fingertip. This allowed the user the feel the objects while grasping them. It was necessary to build an ExoGlove which will be able to also measure joint angles while handling different objects. One more necessity of the Exoglove version 1 was that it was supposed to support the placement of wearable tactile sensors placed on the finger segments.

6.3 ExoGlove Version 1:

The ExoGlove Version 1 provided the user with joint angle information of the user's finger segments along with the provision of measuring of 3-axis tactile forces at the fingertips and finger segments. Other data gloves either provided information related to the tactile forces at the fingertips or data corresponding to the joint angle information between the finger segments. However, the ExoGlove Version 1 allowed the user to

extract multi modular information (tactile + joint angle). Even though this device provided 3-axis tactile data at a single point at the fingertips this device is the first of its kind to provide such comprehensive data, as outlined in this thesis. The ExoGlove Version 1 has its share of drawbacks such as the user was not able to measure tactile forces around different areas of the fingertip. The mechanical design of the ExoGlove Version 1 was bulky. After long usage users complained about the device increasing the muscular fatigue on the user's fingers.

6.4 Necessity of developing a distributed 3-axis tactile sensor:

Human -in-hand manipulation is not just about grasping objects but it is also about also about traversing objects in the human hand workspace. Hence it was realized that the measure tactile forces not just at the single point of the fingertip but also at several points around the fingertips is necessary to understand how humans handle objects. Current wearable tactile sensors only provide tactile data on a single axis. This limited the scope of the tactile sensor only to measure grasping forces.

6.5 FingerTac

To increase the scope of the tactile sensor and to overcome the drawbacks in the currently available wearable sensors, FingerTac was designed. FingerTac was able to measure 3-axis tactile data at several points around the fingertip. This feature of the FingerTac allowed the user to expand the scale of usage from only grasping objects to handling objects. As there are multiple 3-axis distributed sensing points placed around the fingertip area as compared with the currently available wearable tactile sensors, we could realize that FingerTac could provide more richer tactile information with interaction forces while performing in-hand manipulation. These features allow the FingerTac to be the only wearable tactile sensor that can measure distributed 3-axis force over the fingertip area. FingerTac also has the provision to be assembled on Allegro hand. These features make the FingerTac sensor the only available sensor that can be worn on human hands as well as on robot hands.

6.6 The necessity of developing ExoGlove Version 2:

The ExoGlove Version 1 is comprised of a remote center of motion mechanism with multiple joints to perform a revolute motion. To generate a revolute motion a 4-bar linkage design was established. This method was used as one of the objectives of the Exoglove Version 1 was to also support the Wearable Tactile Sensor Version 1 as it was susceptible to loosening after repetitive usage. However, this also led to the ExoGlove Version 1 to be heavy and bulky in operation. To overcome these drawbacks a newer design was required which would be lightweight and easy to operate. Therefore, the ExoGlove Version 2 was realized.

6.7 ExoGlove Version 2:

To track the position and orientation of the FingerTac while being worn on the user's hands an ExoGlove Version 2 was designed. The Exoglove Version 2 comprised of an articulated 4 bar linkage mechanism with each linkage joined together with the corresponding linkage with the help of a revolute joint. A customized magnet-based encoder has been embedded in every revolute joint of the ExoGlove Version 2. The mechanical linkages of the ExoGlove Version 2 were made light weight and with durable ABS plastic to reduce fatigue on the finger while performing in-hand manipulation. The ExoGlove Version 2 is integrated with the FingerTac. Together with the FingerTac ExoGlove Version 2 is the only available wearable device which can measure distributed 3-axis tactile data as well as measure the position and orientation of the fingertips while performing in-hand manipulation of objects.

6.8 Future applications:

As mentioned earlier current exoskeletons or data gloves do not provide multimodal information such as tactile data combined with position data of the finger segments/fingertips. The ExoGlove version 1 and 2 are pioneering devices as they are able to provide combined position as well as tactile data. Further, the ExoGloves can be

utilized to map human hand actions onto the Allegro hand. This can give researchers the scope to explore the potential for skill transfer in forthcoming research.

Moreover, the Exoglove, when integrated with the FingerTac, extends its capabilities by not only measuring forces but also locating the position and orientation of the FingerTac.

6.9 Significance of this Research:

The significance of this technology lies in its potential to unravel the secrets of how artisans manipulate various tools to create intricate works of art. By studying and extracting the nuances of human hand dexterity, researchers aim to gain insights into the intricate skills and techniques employed by artisans. This knowledge is considered a crucial step toward the preservation of a country's rich cultural heritage.

In essence, the technology discussed aims to bridge the gap between the physical actions of the human hand and the artistry it produces. By understanding and preserving these aspects of human dexterity, there is a hope to safeguard and pass down the unique skills and cultural practices associated with craftsmanship, contributing to the preservation and appreciation of a nation's cultural heritage.

Chapter 7

Conclusion and Future works

7.1 Conclusion:

At the beginning of this thesis, we embark on a journey to create a combined distributed 3-axis tactile and position sensing solution to extract the essence of human hand dexterity. In Chapter 3 we initially begin our journey with the wearable tactile sensors for fingertip which have been developed in our lab. This Chapter illustrates the integration of the wearable tactile sensors for human fingertips with the first version of ExoGlove. The ExoGlove Version 1 was a novel design as it is the only available combined wearable 3 axis and position sensing solution which allows the user to directly interact with the object. Direct interaction with the object may seem necessary for some applications however it should be noted that this sensor provides 3 axis tactile information at a single point. Due to the compliant levers enveloping the side of the fingertip it is difficult for the sensor to be used for application which involves the usage of the side of the fingertip such as manipulating an object. For example, traversing a ping pong ball over the surface of the fingertip. To effectively measure the interaction forces of the ping pong ball it is necessary to measure the interaction forces at several area around the fingertip. To address this issue, we explore the new research area which is to create a 3-axis multiple sensing point wearable tactile sensor. Chapter 4 illustrates the development of FingerTac which is a wearable distributed 3-axis tactile sensor. Using this sensor, the user is able to measure interaction forces at not just one but at several areas of the fingertip. This sensor is useful for measuring interaction forces while manipulating several objects by traversing them in 3D space around the fingertip area. Considering the same example as mentioned above the FingerTac will be able to measure interaction forces while traversing the ping pong ball over the surface of the fingertip area. Additionally, FingerTac is also designed such that it is able to be assembled on the Allegro-Hand. This is a novel feature as FingerTac is the only

wearable tactile sensor which can be worn over the robot hand as well as human hand. The interchangeability between human hands and robot hands extends the scope of application for the FingerTac. One of the shortcomings or possible limitation of FingerTac is that it only allows the user to interact with the object indirectly. However, this can be argued that many artisans wear gloves while performing various types of fine manipulation tasks thereby using indirect interaction with the object. Overall, the sensor is able to be worn on human fingertips and can be calibrated to measure 3 axis force at various parts of the fingertip area. Further we believe that this sensor can provide richer information of the interaction forces to the user interacting with the object while wearing the FingerTac. To measure the position and orientation of the FingerTac while manipulating an object Chapter 5 Illustrates the design and development of ExoGlove Version 2. An Encoder is designed and made compact in order to be embedded in a 4 DOF articulated linkage mechanism. This chapter describes the calibration process of the encoder and highlights the system design of the sensor. A Python based visualization software for the kinematics of the ExoGlove has been illustrated and realized. The python code provides visualization of the kinematics in real time allowing the user to measure the position and orientation of the fingertip within the human hand workspace. Further the chapter illustrates the integration methodology used to integrate the encoder along with the previously designed FingerTac to the ExoGlove Version 2. Therefore the ExoGlove Version2 integrated with the FingerTac works as a combined distributed 3-axis and position sensing solution. This combination can be used to measure rich data in a combination of interaction forces and at the same time position data of the FingerTac while manipulating an object. Thereby extracting the three essences of human hand dexterity.

7.1.1 Extracting essence of human hand dexterity:

The FingerTac is able to extract the first essence of human hand dexterity which is measurement of distributed 3-axis force around the fingertip area, while the ExoGlove integrated with the FingerTac is able to locate the position and orientation of the FingerTac there by extracting the third and fourth essence of human hand dexterity. Thus we believe that extraction of human hand dexterity will allow us to understand how artisans handle various tools while creating beautiful works of art and hence is the first step towards preservation of rich cultural heritage of a country.

7.2 Future Works:

In the future, we would like to further develop several aspects of FingerTac as well as ExoGlove Version 2. Some aspects are functional while some are more oriented towards practicality.

7.2.1 FingerTac:

In Chapter 3 we saw that usage of wearable tactile sensor version 1 which allows the user to interact with the object directly. FingerTac allows for in-direct interaction with the object. In the future I would like to make FingerTac more flexible such that the user will be able to feel richer indirect feedback at the user's fingertips.

The existing design of the FingerTac uses the MLX90393 IC which has a large dimension of 3 mm by 3mm. I would like to experiment further by using a smaller Hall-Effect sensor IC to reduce the overall size of the FingerTac.

Currently the Parts used to 3D print the FingerTac are plastic components. In the future I would like to use metal components to increase the robustness of the FingerTac.

7.2.2 Research on skill transfer:

In Chapter 4 we saw that the FingerTac is interchangeable between the human hand and allegro hand. We are currently using uSkin on the Allegro-hand in our lab and performing various kinds of research as illustrated by these research works [6.1], [6.2], [6.3]. Our lab has also worked on research involving in-hand manipulation such as [6.4] and object recognition [6.5].

To train the Allegro Hand we normally employ the Cyberglove which is a widely used data glove. However, the training performed currently is only through teleoperation. Mapping currently involves joint to joint mapping. In the future I would like to assemble the one FingerTac on the Allegro Hand and the other to the users

fingertips. Further I would like to map the location of the FingerTac within the human hand workspace to the Allegro hand workspace using the ExoGlove. I would like to use position control for this process. Next, while holding the object I would like to map the touch states of the FingerTac interacting with the object to the expected touch states of the Allegro Hand. This can be the first step towards skill transfer from human hand to robot hands.

Bibliography

[1.1] PATEL, A.S., 2016. Declining crafts: looking through a different perspective. In: D. HIGGINS and V. DHUPA, eds., In This Place: Cumulus Association Biannual International Conference: conference proceedings, School of Art & Design, Nottingham Trent University, Nottingham, 27 April - 1 May 2016. Nottingham: Nottingham Trent University: CADBE, pp. 292-297. ISBN 9780992887810

[1.2] Sobinov AR, Bensmaia SJ. The neural mechanisms of manual dexterity. Nat Rev Neurosci. 2021 Dec;22(12):741-757. doi: 10.1038/s41583-021-00528-7. Epub 2021 Oct 28. PMID: 34711956; PMCID: PMC9169115.

[1.3] Fotios Alexandros Karakostis, Daniel Haeufle, Ioanna Anastopoulou, Konstantinos Moraitis, Gerhard Hotz, Vangelis Tourloukis, Katerina Harvati, Biomechanics of the human thumb and the evolution of dexterity, Current Biology, Volume 31, Issue 6, 2021, Pages 1317-1325.e8, ISSN 0960-9822,

[1.4] Deflorio Davide, Di Luca Massimiliano, Wing Alan M. ”Skin and Mechanoreceptor Contribution to Tactile Input for Perception: A Review of Simulation Models” Frontiers in Human Neuroscience, 16, 2022, DOI=10.3389/fnhum.2022.862344
ISSN=1662-5161

[1.5] Ritter H, Haschke R. Hands, Dexterity, and the Brain. In: Cheng G PhD, editor. Humanoid Robotics and Neuroscience: Science, Engineering and Society. Boca Raton (FL): CRC Press/Taylor & Francis; 2015. Chapter 3. Available from: https://www.ncbi.nlm.nih.gov/books/NBK299038/

[1.6] Bardo A, Kivell TL, Town K, Donati G, Ballieux H, Stamate C, Edginton T,

Forrester GS. Get a Grip: Variation in Human Hand Grip Strength and Implications for Human Evolution. Symmetry. 2021; 13(7):1142. https://doi.org/10.3390/sym13071142

[1.7] Metcalf Cheryl D., Irvine Thomas A., Sims Jennifer L., Wang Yu L., Su Alvin W. Y., Norris David O. “Complex hand dexterity: a review of biomechanical methods for measuring musical performance”, Frontiers in Psychology, DOI=10.3389/fpsyg.2014.00414, ISSN=1664-1078

[1.8] Toward a Physiological Understanding of Human Dexterity Mario Wiesendanger and Deborah J. Serrien, Physiology 2001 16:5, 228-233

[1.9] Kozbelt A, Durmysheva Y. Lifespan Creativity in a Non-Western Artistic Tradition: A Study of Japanese Ukiyo-E Printmakers. The International Journal of Aging and Human Development. 2007;65(1):23-51. doi:10.2190/166N-6470-1325-T341

[2.1] D. J. Beebe, D. D. Denton, R. G. Radwin, and J. G. Webster, “A silicon-based tactile sensor for finger-mounted applications,” IEEE Transactions on Biomedical Engineering, vol. 45, no. 2, pp. 151–159, Feb. 1998.

[2.2] Z. Huang, F. Sun, H. Min, B. Fang, W. Zhang, and X. Hu, “A novel wearable tactile sensor array designed for fingertip motion recognition,” in 2017 IEEE International Conference on Robotics and Biomimetics (ROBIO), 2017, pp. 165–170.

[2.3] Y. Wang, Y. Lu, D. Mei, and G. Qiang, “Development of wearable tactile sensor based on galinstan liquid metal for both temperature and contact force sensing,” in 2020 IEEE 16th International Conference on Automation Science and Engineering (CASE), 2020, pp. 442–448.

[2.4] Y. Hasegawa, M. Shikida, D. Ogura and K. Sato, "Glove Type of Wearable Tactile Sensor Produced by Artificial Hollow Fiber," TRANSDUCERS 2007 - 2007 International Solid-State Sensors, Actuators and Microsystems Conference, Lyon, France, 2007, pp. 1453-1456, doi: 10.1109/SENSOR.2007.4300418.

[2.5] M. Bianchi, R. Haschke, G. Buscher, S. Ciotti, N. Carbonaro, ¨ and A. Tognetti, “A multi-modal sensing glove for human manualinteraction studies,” Electronics, vol. 5, no. 3, 2016. [Online]. Available: https://www.mdpi.com/2079-9292/5/3/42.

[2.6] Subramanian Sundaram et al., “Learning the signatures of the human grasp using a scalable tactile glove,” Nature, 569 (7758), 2019.

[2.7] E. Battaglia, M. Bianchi, A. Altobelli, G. Grioli, M. G. Catalano, A. Serio, M. Santello, and A. Bicchi, “Thimblesense: A fingertip wearable tactile sensor for grasp analysis,” IEEE Transactions on Haptics, vol. 9, no. 1, pp. 121–133, Jan 2016.

[2.8] E. Battaglia, M. G. Catalano, G. Grioli, M. Bianchi, and A. Bicchi, “Exosense: Measuring manipulation in a wearable manner,” in 2018 IEEE International Conference on Robotics and Automation (ICRA), 2018, pp. 2774–2781.

[2.9] H. Kristanto, P. Sathe, A. Schmitz, T. P. Tomo, S. Somlor, and S. Sugano, “A wearable three-axis tactile sensor for human fingertips,” IEEE Robotics and Automation Letters, vol. 3, no. 4, pp. 4313–4320, Oct 2018.

[2.10] H. Kristanto, P. Sathe, C. Hsu, A. Schmitz, T. P. Tomo, S. Somlor, and S. Sugano, “Development of a 3-axis human fingertip tactile sensor with an ortho-planar spring,” in 2019 IEEE International Conference on Robotics and Biomimetics (ROBIO), 2019, pp. 297–302.

[2.11] H. Kristanto, P. Sathe, A. Schmitz, C. Hsu, T. P. Tomo, S. Somlor, and S. Sugano, “Development of a 3-axis human fingertip tactile sensor based on distributed hall effect sensors,” in 2019 IEEE-RAS 19th International Conference on Humanoid Robots (Humanoids), 2019, pp. 1–7.

[2.12] P. Sathe, A. Schmitz, H. Kristanto, C. Hsu, T. P. Tomo, S. Somlor, and S. Shigeki, “Development of ExoGlove for measuring 3-axis forces acting on the human finger without obstructing natural human-object interaction,” in 2020 IEEE/RSJ International Conference on Intelligent Robots and Systems (IROS), 2020, pp. 4106–4113.

[2.13] E. R. Serina, C. Mote, and D. Rempel, “Force response of the fingertip pulp to

repeated compression – effects of loading rate, loading angle and anthropometry," Journal of Biomechanics, vol. 30, no. 10, pp. 1035–1040, Oct. 1997. [2.14] E. R. Serina, E. Mockensturm, C. D. Mote Jr., and D. Rempel, "A structural model of the forced compression of the fingertip pulp," Journal of Biomechanics, vol. 31, no. 7, pp. 639–646, Jul. 1998.

[2.15] Y. Matsuura, S. Okamoto, and Y. Yamada, "Estimation of Finger Pad Deformation Based on Skin Deformation Transferred to the Radial Side," in Haptics: Neuroscience, Devices, Modeling, and Applications, ser. Lecture Notes in Computer Science. Springer, Berlin, Heidelberg, Jun. 2014, pp. 313–319.

[2.16] A. G. Perez, G. Cirio, D. Lobo, F. Chinello, D. Prattichizzo, and M. A. Otaduy, "Efficient nonlinear skin simulation for multi-finger tactile rendering," in 2016 IEEE Haptics Symposium (HAPTICS), 2016, pp. 155–160.

[2.17] M. Nakatani, T. Kawasoe, K. Shiojima, K. Koketsu, S. Kinoshita, and J. Wada, "Wearable contact force sensor system based on fingerpad deformation," in 2011 IEEE World Haptics Conference, Jun. 2011, pp. 323–328.

[3.1] P. Sathe H. Kristanto, "Compliant Joint Mechanism for 3 axis Human Fingertip tactile Sensor Based on Distributed Hall Effect Sensors," RSJ conference Sept 2019.

[3.2] M. Gaafar, M. Magdy, A. T. Elgammal, A. El-Betar and A. M. Saeed, "Development of a New Compliant Remote Center of Motion (RCM) Mechanism for Vitreoretinal Surgery," 2020 6th International Conference on Control, Automation and Robotics (ICCAR), Singapore, 2020, pp. 183-187, doi: 10.1109/ICCAR49639.2020.9108005.

[3.3] R. S. Bobade and S. K. Yadav, "Compliant Remote Center Motion Mechanism for Minimally Invasive Surgical Robots," 2018 3rd International Conference for Convergence in Technology (I2CT), Pune, India, 2018, pp. 1-5, doi: 10.1109/I2CT.2018.8529460.

[3.4] H. M. Yip, P. Li, D. Navarro-Alarcon, Z. Wang and Y. -h. Liu, "A new circular-guided remote center of motion mechanism for assistive surgical robots," 2014 IEEE International Conference on Robotics and Biomimetics (ROBIO 2014), Bali, Indonesia,

2014, pp. 217-222, doi: 10.1109/ROBIO.2014.7090333.

[3.5] Y. Fu, G. Niu, B. Pan, K. Li and S. Wang, "Design and optimization of remote center motion mechanism of Minimally Invasive Surgical robotics," *2013 IEEE International Conference on Robotics and Biomimetics (ROBIO)*, Shenzhen, China, 2013, pp. 774-779, doi: 10.1109/ROBIO.2013.6739556.

[3.6] C. -B. Chng, B. Duan and C. -K. Chui, "Modeling and simulation of a Remote Center of Motion mechanism," *2016 IEEE Region 10 Conference (TENCON)*, Singapore, 2016, pp. 1755-1758, doi: 10.1109/TENCON.2016.7848320.

[3.7] N. Miyata, M. Kouch, M. Mochimaru and T. Kurihara, "Finger joint kinematics from MR images," *2005 IEEE/RSJ International Conference on Intelligent Robots and Systems*, Edmonton, AB, Canada, 2005, pp. 2750-2755, doi: 10.1109/IROS.2005.1545611.

[3.8] C. HSU et al., "Implementation of a Remote Center of Motion Robot Finger with Tactile Sensors in the Joints," 2019 IEEE International Conference on Robotics and Biomimetics (ROBIO), Dali, China, 2019, pp. 247-252, doi: 10.1109/ROBIO49542.2019.8961450.

[3.9] G. Khullar, A. Schmitz, C. Hsu, P. Sathe, S. Funabashi and S. Sugano, "A Multi-Fingered Robot Hand with Remote Center of Motion Mechanisms for Covering Joints with Soft Skin," 2021 IEEE International Conference on Robotics and Biomimetics (ROBIO), Sanya, China, 2021, pp. 564-570, doi: 10.1109/ROBIO54168.2021.9739600.

[3.10] Shuanghui Hao, Yong Liu and Minghui Hao, "Study on a novel absolute magnetic encoder," *2008 IEEE International Conference on Robotics and Biomimetics*, Bangkok, 2009, pp. 1773-1776, doi: 10.1109/ROBIO.2009.4913270.

[3.11] S. -M. Huang, P. -Y. Gi and P. -Y. Wu, "A Design of Wearable Goniometers for Measuring Carpal Angular Movement," *2018 IEEE International Conference on Advanced Manufacturing (ICAM)*, Yunlin, Taiwan, 2018, pp. 1-4, doi: 10.1109/AMCON.2018.8615058.

[4.1] T. P. Tomo, S. Somlor, A. Schmitz, S. Hashimoto, S. Sugano, and

L. Jamone, “Development of a hall-effect based skin sensor,” in 2015
IEEE SENSORS, 2015, pp. 1–4.

[4.2] T. P. Tomo, W. K. Wong, A. Schmitz, H. Kristanto, A. Sarazin, L. Jamone, S. Somlor, and S. Sugano, “A modular, distributed, soft, 3-axis sensor system for robot hands,” in 2016 IEEE-RAS 16th International Conference on Humanoid Robots (Humanoids), 2016,
pp. 454–460.

[4.3] T. P. Tomo, A. Schmitz, W. K. Wong, H. Kristanto, S. Somlor, J. Hwang, L. Jamone, and S. Sugano, “Covering a robot fingertip with uskin: A soft electronic skin with distributed 3-axis force sensitive elements for robot hands,” IEEE Robotics and Automation Letters, vol. 3, no. 1, pp. 124–131, 2018.

[4.4] T. P. Tomo, M. Regoli, A. Schmitz, L. Natale, H. Kristanto, S. Somlor, L. Jamone, G. Metta, and S. Sugano, “A new silicone structure for uskin—a soft, distributed, digital 3-axis skin sensor and its integration on the humanoid robot icub,” IEEE Robotics and Automation Letters, vol. 3, no. 3, pp. 2584–2591, 2018.

[4.5] I. M. Bullock, T. Feix and A. M. Dollar, "Analyzing human fingertip usage in dexterous precision manipulation: Implications for robotic finger design," *2014 IEEE/RSJ International Conference on Intelligent Robots and Systems*, Chicago, IL, USA, 2014, pp. 1622-1628, doi: 10.1109/IROS.2014.6942772.

[5.1] X. Gu, Y. Zhang, W. Sun, Y. Bian, D. Zhou, and P. O. Kristensson, “Dexmo: An inexpensive and lightweight mechanical exoskeleton for motion capture and force feedback in vr,” Proceedings of the 2016 CHI Conference on Human Factors in Computing Systems, 2016.

[5.2] Y.-H. Lee, M. Kim, H.-Y. Kim, D. Lee, and B.-J. You, “Chicap: low-cost hand motion capture device using 3d magnetic sensors for manipulation of virtual objects,” ACM SIGGRAPH 2018 Emerging Technologies, 2018.

[5.3] G. D. Kessler, L. F. Hodges, and N. Walker, “Evaluation of the cyberglove as a whole-hand input device,” ACM Trans. Comput.-Hum. Interact., vol. 2, no. 4, p. 263–283, dec 1995. [Online]. Available:https://doi.org/10.1145/212430.212431

[5.4] D. Sim, Y. Baek, M. Cho, S. Park, A. S. M. S. Sagar, and H. S. Kim, “Low-latency haptic open glove for immersive virtual reality interaction,” Sensors, vol. 21, no. 11, 2021. [Online]. Available: https://www.mdpi.com/1424-8220/21/11/3682

[6.1] S. Funabashi et al., "Multi-Fingered In-Hand Manipulation With Various Object Properties Using Graph Convolutional Networks and Distributed Tactile Sensors," in IEEE Robotics and Automation Letters, vol. 7, no. 2, pp. 2102-2109, April 2022, doi: 10.1109/LRA.2022.3142417.

[6.2] S. Funabashi et al., "Stable In-Grasp Manipulation with a Low-Cost Robot Hand by Using 3-Axis Tactile Sensors with a CNN," 2020 IEEE/RSJ International Conference on Intelligent Robots and Systems (IROS), Las Vegas, NV, USA, 2020, pp. 9166-9173, doi: 10.1109/IROS45743.2020.9341362.

[6.3] S. Funabashi et al., "Variable In-Hand Manipulations for Tactile-Driven Robot Hand via CNN-LSTM," 2020 IEEE/RSJ International Conference on Intelligent Robots and Systems (IROS), Las Vegas, NV, USA, 2020, pp. 9472-9479, doi: 10.1109/IROS45743.2020.9341484.

[6.4] S. Funabashi, A. Schmitz, S. Ogasa and S. Sugano, "Morphology Specific Stepwise Learning of In-Hand Manipulation With a Four-Fingered Hand," in IEEE Transactions on Industrial Informatics, vol. 16, no. 1, pp. 433-441, Jan. 2020, doi: 10.1109/TII.2019.2893713.

[6.5] S. Funabashi et al., "Object Recognition Through Active Sensing Using a Multi-Fingered Robot Hand with 3D Tactile Sensors," 2018 IEEE/RSJ International Conference on Intelligent Robots and Systems (IROS), Madrid, Spain, 2018, pp. 2589-2595, doi: 10.1109/IROS.2018.8594159.